

The Greenhouse Effect and Climate Change

Stephen E Schwartz¹

¹Affiliation not available

November 21, 2022

Abstract

Earth's greenhouse effect is manifested as the difference between thermal infrared radiation emitted at the Earth surface and that emitted to space at the top of the atmosphere. This difference is due mainly to absorption and downward emission of radiant energy by atmospheric trace gases. The greenhouse effect is an essential feature of Earth's climate system that results in global mean surface temperature about 32 K greater than it would otherwise be for the same planetary absorption of solar radiation. Increases in atmospheric carbon dioxide, methane, nitrous oxide, and chlorofluorocarbons due to human activities over the past 200 years have increased the greenhouse effect by about 1% relative to the radiative fluxes that drive the climate system. The resultant increase in global temperature and other changes in climate are of great societal concern. This article introduces the physics of the greenhouse effect and more broadly of Earth's climate system and of climate change and provides resources for further study. It reviews the processes responsible for the greenhouse effect, the anthropogenic increase in the greenhouse effect, and the response of the climate system to this increase. Developing prognostic capability to determine this response to an accuracy that would be useful to inform policymaking is the major challenge facing climate scientists today.

The Greenhouse Effect and Climate Change

Stephen E. Schwartz

Environmental and Climate Sciences, Brookhaven National Laboratory, Upton NY 11973; ses@bnl.gov

ABSTRACT. Earth's greenhouse effect is manifested as the difference between thermal infrared radiation emitted at the Earth surface and that emitted to space at the top of the atmosphere. This difference is due mainly to absorption and downward emission of radiant energy by atmospheric trace gases. The greenhouse effect is an essential feature of Earth's climate system that results in global mean surface temperature about 32 K greater what it would otherwise be for the same planetary absorption of solar radiation. Increases in atmospheric carbon dioxide, methane, nitrous oxide, and chlorofluorocarbons due to human activities over the past 200 years have increased the greenhouse effect by about 1% relative to the radiative fluxes that drive the climate system. The resultant increase in global temperature and other changes in climate are of great societal concern. This article introduces the physics of the greenhouse effect and more broadly of Earth's climate system and of climate change and provides resources for further study. It reviews the processes responsible for the greenhouse effect, the anthropogenic increase in the greenhouse effect, and the response of the climate system to this increase. Developing prognostic capability to determine this response to an accuracy that would be useful to inform policymaking is the major challenge facing climate scientists today.

Copyright © 2018, Brookhaven Science Associates, LLC, Brookhaven National Laboratory. The U.S. Government is granted for itself and others acting on its behalf a paid-up, nonexclusive, irrevocable worldwide license in this preprint to reproduce, prepare derivative works, distribute copies to the public, and perform publicly and display publicly by or on behalf of the Government.

I. INTRODUCTION

The so-called “greenhouse effect” is essential to maintaining a climate that is hospitable to life on Earth, as we know it. This article describes both the natural greenhouse effect and the increase in the greenhouse effect due to human activity, denoted here the *intensified greenhouse effect*. This intensified greenhouse effect is a major contributor to the change in Earth’s climate that has occurred over the industrial era and is expected to continue over at least the next several centuries. As the greenhouse effect exerts a major effect on Earth’s radiation budget, it is necessary to quantify the several fluxes that contribute to this budget to provide context.

Before examining Earth’s greenhouse effect, it may be instructive to consider a paradox regarding the energy budget of a human being. The nominal standard daily energy intake for an adult, 2000 Calories, corresponds to $8.4 \times 10^6 \text{ J}\cdot\text{day}^{-1}$ or 100 W. Now consider a human being as a blackbody radiator; an emissivity of unity is a good approximation in the thermal infrared region of the electromagnetic spectrum. For a body temperature of 37°C or 310 K the emitted radiative flux density is about $500 \text{ W}\cdot\text{m}^{-2}$ as given by the Stefan-Boltzmann radiation law, σT^4 , where σ is the Stefan-Boltzmann radiation constant, $\sim 5.67 \times 10^{-8} \text{ W}\cdot\text{m}^{-2}\cdot\text{K}^{-4}$. Approximating the human body as a cylinder and calculating the surface area of an adult as 1 m^2 (2-m high \times 0.5 m circumference) results in an emitted power of 500 W, well more than the caloric intake. How can this be? To resolve this apparent paradox imagine a person standing outside at the South Pole at night in the polar winter without clothes. Very quickly, that person will freeze to death. So why are we not freezing to death wearing clothes at ordinary temperatures? We are still radiating 500 W, but our environment is radiating back at us. If our clothes are at a temperature close to body temperature, the net rate of loss of energy by radiation is a small fraction of the gross radiation

rate calculated by the Stefan-Boltzmann law. On a warm day, even when wearing little clothing, one is receiving and absorbing radiant energy from the surrounding atmosphere and from the Earth surface and any nearby structures, so that again the net rate of energy radiated by one's body is much less than the gross Stefan-Boltzmann rate.

The phenomenon just described is entirely analogous to what takes place in Earth's climate system. Shortwave solar radiation from the Sun transmitted through the largely transparent atmosphere reaches the surface of the planet, where it is absorbed, heating the surface. As detailed below, the gross radiative flux density emitted by the surface of the planet (land, water) greatly exceeds, on global and annual average, the input radiative flux density received from the Sun, just as the thermal infrared radiation emitted by a person greatly exceeds his or her caloric intake. The radiation emitted by the surface of the planet in the thermal infrared, where the atmosphere is much less transparent, is absorbed by the atmosphere, which is thereby heated and in turn radiates, in part downward toward the surface. This *downwelling* infrared radiation from the atmosphere to the surface greatly diminishes the net upward infrared flux from the surface relative to the gross blackbody flux. This phenomenon is called the greenhouse effect, based on the erroneous supposition that a greenhouse maintains its warmth by absorption and downward emission of longwave radiation from the glass surfaces. (Actual greenhouses maintain their warm temperature mainly by the enclosure's suppression of convective transport of warm air away from the surface¹) Thus, just as infrared radiation from the environment to an individual resolves the paradox of emitted radiation greatly exceeding caloric intake, infrared radiation from the atmosphere to the surface resolves the paradox of the thermal infrared radiation emitted by the surface greatly exceeding the incoming solar radiative flux.

This article examines the greenhouse effect and the intensified greenhouse effect, the increase in the greenhouse effect induced by human activities over the so-called Anthropocene epoch. The latter term was proposed by Paul Crutzen, 1995 Nobelist for atmospheric chemistry, to characterize the epoch of Earth's geological history that began with industrialization more or less 200 years ago.^{2,3} Examination of the greenhouse effect requires considerable understanding of Earth's climate and the processes that control it, but the emphasis here is on the perturbations that induce climate change and the responses to these perturbations. The focus here is physical processes, but these cannot be separated from chemical and biological processes. Nonetheless, much insight is gained by looking at the climate system as a physical system. The focus here is on quantities such as the global scale radiation budget, the greenhouse effect and its influence on surface temperature, perturbations in the global radiation budget due to the incremental amounts of atmospheric infrared-active gases (greenhouse gases or GHGs) resulting from human activities, and resulting perturbations in temperature. Here the index of climate change is mainly change in global and annual mean near-surface air temperature (commonly denoted global mean surface temperature, GMST); this use of change in GMST as a surrogate for climate change requires some justification. The focus on GMST is due in part to the iconic status of this quantity as a single index of climate change and in part to the expectation that to first order other changes in climate would depend parametrically on change in GMST.

Sources and References. A broad examination of present understanding of the climate system and climate change is given in the several Assessment Reports of Working Group I of the Intergovernmental Panel on Climate Change (IPCC). The most recent report, the Fifth,⁴ was published in 2013; the Fourth report⁵ occasioned award of the Nobel Peace Prize to the IPCC. These reports, which are freely downloadable on the web, are essential references for any

student of climate and climate change. Citations are given throughout this article to pertinent sections of these reports. Several texts that might serve as an introduction to the climate and to the physics of climate are noted in the References to this section. A hypertext history of the development of understanding of the greenhouse effect and climate change more generally by Weart,⁶ which supplements his very readable book, or which can be used as a stand-alone, may be accessed at <http://www.aip.org/history/climate/index.htm>. Citations to the primary and secondary literature given in this article are intended to be of historical and pedagogical value, as well as to lead the reader to the research literature without attempting to be exhaustive. Links are also provided to some key data sets.

A word about uncertainties: Uncertainties are quite large in many key quantities pertinent to climate change. To provide a systematic characterization of uncertainties the IPCC (Ref [4], Box TS-1) has adopted a nomenclature, wherein square brackets are used to indicate the range that is expected to encompass the central 90% of the likelihood distribution (5 to 95)% for the value of the quantity in question, denoted the “very likely” range (approximately $\pm 1.6\sigma$ for a Gaussian probability distribution function). The central 66% of the likelihood distribution (approximately $\pm 1\sigma$) is denoted the “likely” range for the quantity. This notation and terminology is employed here when quoting such ranges. Because of the large uncertainties, it is sometimes useful to report the ratio of the end members of the “likely” or “very likely” ranges, denoted, for example, by the phrase “a factor of 3.”

Organization of this Article. Section II presents an overview of Earth’s radiation budget and emphasizes that to good approximation Earth’s climate system can be characterized as a steady state. Section III provides a brief overview of Earth’s climate system with emphasis on thermal structure of the atmosphere as a function of altitude pertinent to the greenhouse effect. Section

IV deals with the role of the greenhouse effect on Earth's climate and identifies the key GHGs. Section V introduces the concept of radiative forcing of climate change, that is, imposed changes on the planetary radiation budget, changes that would be expected to alter Earth's climate. Section VI focuses on increases in greenhouse gases over the Anthropocene epoch and the resultant radiative forcings. Section VII describes climate system response to forcing and introduces the climate sensitivity concept. Section VIII relates forcings to observed temperature changes and examines implications. A brief summary is given in Section IX. Several Supplementary Notes (SN) that provide detail or lend perspective are provided.

1. "Note on the Theory of the Greenhouse," R. W. Wood, *Philosophical Magazine* **17**, 319-320 (1909). Historical and popular interest; might serve as basis for laboratory experiment. (E)
2. "The Anthropocene," P. J. Crutzen and E. F. Stoermer, *IGPP Newsletter* No. 41, pp. 16-18 (2000). <http://igbp.sv.internetborder.se/download/18.316f18321323470177580001401/1316517410973/NL41.pdf>. Historical. (E)
3. "Geology of mankind," P. J. Crutzen, *Nature* **415**, 23-23 (2002). Historical and influential commentary. (E)
4. **Climate Change 2013: The Physical Science Basis (AR5)**, T. F. Stocker, D Qin, G.-K. Plattner, M. Tignor, S. K. Allen, J. Boschung, A. Nauels, Y Xia, V. Bex and P. M. Midgley, Editors (Cambridge University Press, Cambridge, United Kingdom and New York, NY, 2013). http://www.climate2013.org/images/report/WG1AR5_ALL_FINAL.pdf. Intergovernmental Panel on Climate Change. Essential reference. (E)-(I).

- 5. Climate Change 2007: The Physical Science Basis (AR4)**, S. Solomon, D. Qin, M. Manning, Z. Chen, M. Marquis, K. B. Averyt, M. Tignor and H. L. Miller (Editors). (Cambridge University Press, Cambridge, United Kingdom and New York, NY, 2007). http://www.ipcc.ch/publications_and_data/ar4/wg1/en/contents.html. Intergovernmental Panel on Climate Change. Essential reference. (E)-(I).
- 6. The Discovery Of Global Warming: Revised And Expanded Edition**, Spencer R. Weart (Harvard University Press, 2008). Good introduction to climate, greenhouse effect, and intensified greenhouse effect. (E)
- 7. Global Warming: The Hard Science**, L. D. D. Harvey (Prentice Hall, London, 2000). Very approachable introduction to climate change. (E)-(I).
- 8. The Physics of Atmospheres, Third Edition**, J. T. Houghton (Cambridge University Press, Cambridge, 2002). Good starting point for physics students wishing to delve into atmospheric physics. (E)-(A).
- 9. An Introduction to Atmospheric Radiation, Second Edition**, K. N. Liou (Academic Press, 2002). Treats not only atmospheric radiation but also the properties of Earth's atmosphere that influence radiation transfer; also contains an extensive treatment of climate change. (E)-(A).
- 10. Physics of Climate**, J. P. Peixoto and A. H. Oort (Am. Inst. of Phys., New York, 1992). Another good starting point for physics students wishing to delve into atmospheric physics. (E)-(A).

II. OVERVIEW OF EARTH'S RADIATION BUDGET

A. Top-of-atmosphere budget

Earth's climate, a dynamic, chaotic, near-steady-state system, is driven almost entirely by absorption of solar energy. This energy heats the planet and is responsible for climate and weather: wind, ocean currents, rain and snow, and temperature. "Near steady state" means that the energy introduced into the system is balanced, almost exactly, by energy leaving the system. Here and throughout this article phrases such as "almost exactly" mean that the difference is very small relative to the quantity of interest. However, climate change is a consequence of, or is characterized by, such small differences. Satellite measurements confirm, on global and annual average, the near equality of the absorbed power, energy from the Sun, commonly denoted as *shortwave energy*, and the emitted power, energy in the thermal infrared, *longwave energy*. Conveniently, these two spectral ranges, calculated according to the *Planck radiation law* for black bodies¹¹ (Max Planck; Nobel, 1918) at temperatures 5770 K and 255 K, respectively, are almost completely non-overlapping (Figure 1), simplifying the discussion and facilitating measurements of the different components. For the rate of absorption of solar energy, normalized to the surface area of the planet, denoted Q , and for the rate of emission of thermal infrared energy, similarly normalized, denoted $-E$ (the sign convention is that positive denotes heat *into* the climate system), then to good approximation on global and annual average,

$$Q + E = 0; \tag{1}$$

that is, the system is approximately in steady state, with the magnitudes of the individual terms greatly exceeding the net rate of energy uptake or loss.

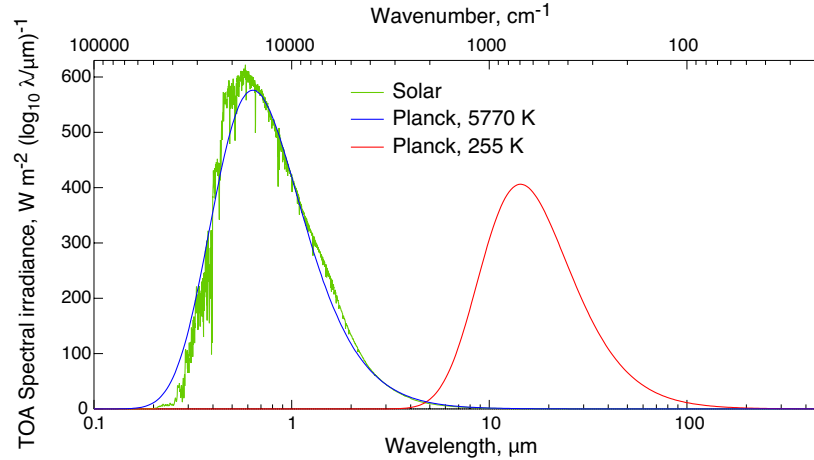


Figure 1. Spectral distribution of downwelling shortwave and upwelling longwave irradiance at the top of the atmosphere as calculated using the Planck radiation law for black bodies at 5770 K (normalized to $340 \text{ W}\cdot\text{m}^{-2}$) and 255 K (normalized to $240 \text{ W}\cdot\text{m}^{-2}$) versus wavelength or wavenumber (upper and lower axes, respectively, logarithmic scale). Also shown for comparison is measured spectral solar irradiance¹² at mean Earth-Sun distance, divided by 4 to correspond to global-mean irradiance.

The rate of energy absorption Q is very nearly equal to the 1/4 times the so-called “solar constant,” J_S , times the planetary co-albedo, γ :

$$Q = \gamma J_S / 4. \quad (2)$$

The factor of 1/4 is geometric, the ratio of the area of the planet to that of the subtended disk being almost exactly 4. The *co-albedo*, γ , is the complement of the planetary albedo, where the planetary *albedo* (more formally, Bond albedo¹³), is the fraction, over the illuminated hemisphere, of incident solar irradiance that is reflected (more strictly, scattered) back to space. Viewed from space Earth is not black: clouds and deserts are bright; oceans and forests are dark. The mean planetary albedo, determined by satellite measurements,^{14,15} is about 0.29. The solar constant, J_S , is the flux density (hereinafter, flux) of solar irradiance at the mean Earth-Sun distance. For the measured value of the solar constant about $1360 \text{ W}\cdot\text{m}^{-2}$,¹⁶ the absorbed power Q is thus about $240 \text{ W}\cdot\text{m}^{-2}$. Within measurement accuracy, the emitted longwave power is also about $240 \text{ W}\cdot\text{m}^{-2}$.¹⁵ Considering the planet as a black body in the thermal infrared permits a

radiative temperature, T_{toa} , at the top of the atmosphere (TOA), to be calculated by the Stefan Boltzmann radiation law,

$$E = -\sigma T_{\text{toa}}^4; T_{\text{toa}} = (-E / \sigma)^{1/4}. \quad (3)$$

Solving for T_{toa} gives about 255 K. This is the temperature that one would ascribe to the planet if measuring its thermal emission from space, from which one would infer that Earth is a frozen planet.

The difference (32 K) between the radiative temperature of the planet, 255 K, and the global mean surface temperature (GMST, T_s), 287 K, is a consequence, or measure, of Earth's greenhouse effect. The paradox, that the emitted flux at the surface exceeded the absorbed radiant energy, was recognized by Fourier as early as the 1820's. Fourier correctly attributed the elevated temperature at Earth's surface at least in part to the lack of transparency of the atmosphere to thermal radiation, in contrast to its transparency to visible radiation.¹⁷ This hypothesis was confirmed by Tyndall,¹⁸ who established that downward emission of infrared radiation is due to trace gases in the atmosphere, principally water vapor and carbon dioxide. Tyndall drew the analogy that "As a dam built across a river causes a local deepening of the stream, so our atmosphere, thrown as a dam across the terrestrial rays, produces a local heightening of the temperature at the earth's surface." Thermal infrared radiation emitted at the surface is absorbed by infrared-active gases aloft in the atmosphere (and by clouds). These gases and clouds also emit in the thermal infrared; some of the emitted power is returned to the surface of the planet, increasing the total power absorbed at the surface well beyond the absorbed shortwave, thus increasing the surface temperature to a value greater than it would be absent this greenhouse effect.

B. Global energy balance

As stated in Eq. (1) and indicated in Figure 2 the global, annual average of the longwave irradiance emitted at the TOA is virtually equal to that of the absorbed shortwave irradiance. There is a very slight imbalance even in the natural climate system at steady state due to non-radiative energy sources, mainly natural radioactive decay and release of gravitational potential energy of the solid earth. More importantly, the energy imbalance of the planet is confidently thought to have been affected by changes in atmospheric composition over the past 250 years or so. In principle, the net energy uptake by the planet might be measured from space as the difference between absorbed shortwave and emitted longwave radiation integrated over the planet,

$$N \equiv Q + E = (J_S / 4 - J_{sw\uparrow}) - J_{lw\uparrow}. \quad (4)$$

However the energy imbalance is well less than the accuracy of satellite measurements at present (about $\pm 3 \text{ W}\cdot\text{m}^{-2}$),¹⁴ so the assertion of global near equality of absorbed shortwave irradiance and emitted longwave irradiance rests more on understanding the consequences of an imbalance than on measurement (**SN1**). From measurements mainly of the change of ocean temperature over the past several decades, integrated spatially over the world ocean to give change in ocean heat content, it is estimated that the net planetary energy imbalance is about $0.5 \text{ W}\cdot\text{m}^{-2}$ (Ref.[4], Box 3.1). Natural internal variability of the climate system such as the El Niño–Southern Oscillation gives rise to fluctuations in the net energy budget on several-year to perhaps multi-decadal time scales. Naturally caused fluctuations are also induced by identified causes such as variation in solar irradiance and changes in planetary shortwave reflectance due to short-lived increases stratospheric aerosols (suspensions of microscopic or submicroscopic particles) resulting from large, impulsive volcanic emissions

C. Earth's energy budget

Global and annual means of the several fluxes that comprise Earth's energy budget are averages of quantities that vary greatly in space and time. Current estimates of these fluxes are shown in Figure 2. The global mean thermal infrared radiative flux emitted at the surface, calculated by the Stefan-Boltzmann radiation law for GMST 287 K with emissivity taken as unity, is $385 \text{ W}\cdot\text{m}^{-2}$, substantially greater than the absorbed shortwave radiation and greater even than the incident shortwave radiation at the TOA. One measure of the greenhouse effect is the difference between longwave flux emitted at the surface and that exiting at the top of the atmosphere, $\sim 145 \text{ W}\cdot\text{m}^{-2}$. The radiative flux from the surface is augmented by a further $110 \text{ W}\cdot\text{m}^{-2}$ by transfer of latent heat (evaporation of water that condenses in the atmosphere and is returned to the surface as liquid or solid precipitation) and sensible heat (enthalpy, transferred by conduction and/or convection). Much of the power emitted at the surface is returned to the surface by downwelling longwave radiation from the atmosphere to the surface. Referring the emitted longwave energy flux at the TOA, $-E$, to the GMST, T_s , permits definition of an *effective emissivity* of the planet ϵ such that

$$-E = \epsilon \sigma T_s^4 . \quad (5)$$

For the surface emitted flux $385 \text{ W}\cdot\text{m}^{-2}$ and $-E = 240 \text{ W}\cdot\text{m}^{-2}$, the effective planetary emissivity, $\epsilon = 0.62$. This emissivity is likewise a measure of the magnitude of Earth's greenhouse effect. These considerations abundantly establish the importance of the greenhouse effect in Earth's climate system.

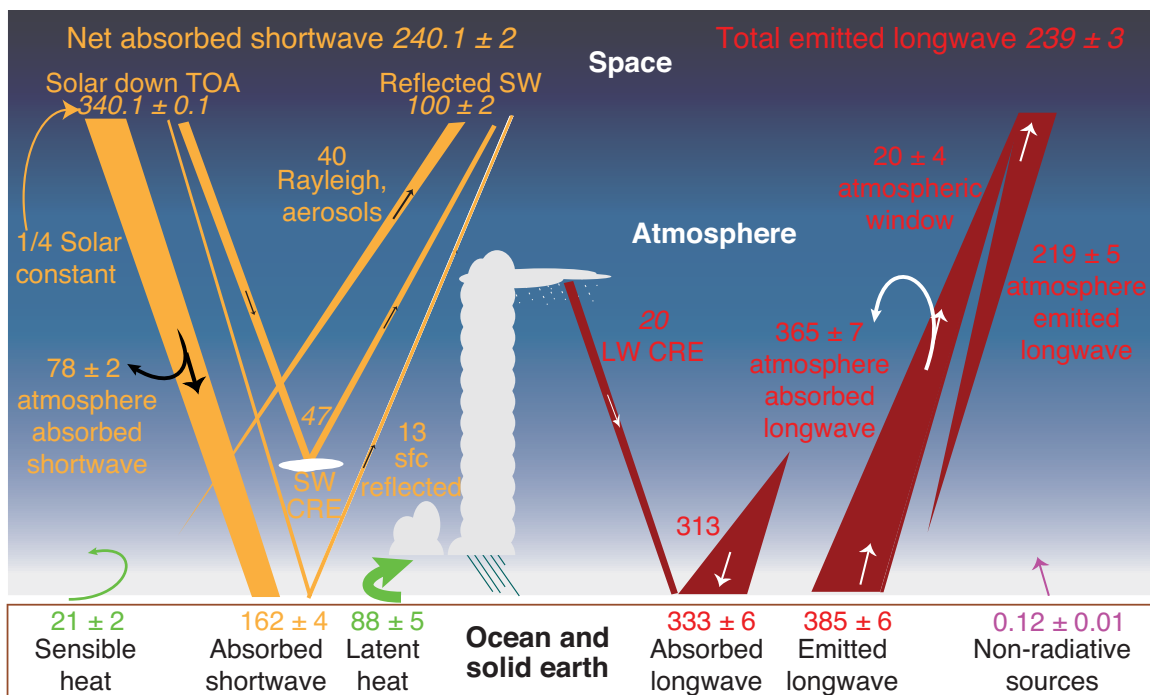


Figure 2. Energy flows in Earth's climate system. Quantities shown are global and annual mean energy fluxes ($\text{W}\cdot\text{m}^{-2}$) between the atmosphere and space, and between the atmosphere and the Earth surface. Satellite-measured quantities and associated uncertainties are in italics; remaining fluxes are calculated, with subjective $1\text{-}\sigma$ uncertainty estimates. Shortwave (solar) fluxes are shown in tan; longwave (thermal infrared) fluxes in red; sensible and latent heat from surface to atmosphere in green; non-radiative sources (natural radioactive decay, gravitational collapse, fossil fuel combustion, nuclear energy) in magenta. TOA, top of atmosphere; SW, shortwave; LW, Longwave; CRE, cloud radiative effect; sfc, surface. Modified from Ref. [19].

Also shown in Figure 2 are estimates of the $1\text{-}\sigma$ uncertainties in the several flux terms; historically such uncertainty estimates have proved to be optimistic¹⁹, as subsequent research leads to improved measurements and understanding. Nonetheless, the climate system must be considered to be in very close energy balance at the top of the atmosphere, in the atmosphere itself, and in the upper, mixed layer of the world ocean.

Although depictions of global and annual mean energy fluxes such as Figure 2 are useful to set the scene by showing the magnitudes of these fluxes, they do not display the large variability characteristic of these quantities. The several terms in Earth's energy budget exhibit substantial

seasonal variation, up to $15 \text{ W}\cdot\text{m}^{-2}$, even at global mean, a consequence mainly of the eccentricity of the Earth orbit and hemispheric asymmetry in oceans. In contrast, the interannual variability is quite small, less than $1 \text{ W}\cdot\text{m}^{-2}$ over a decade of high quality measurements from space (Ref.[14]; <http://ceres-tool.larc.nasa.gov/ord-tool/jsp/EBAFSelection.jsp>) a measure of the constancy of the climate system on this time scale. Any changes in Earth's climate in response to externally imposed perturbations would be manifested in changes in the several radiation terms in addition to changes in surface temperature and ocean heat content. These seasonal variations, which are large compared to the forcings that have been imposed on the climate system over the Anthropocene epoch, serve as further backdrop for examination of climate change and are indicative of measurement and modeling challenges that face the climate change research community.

Radiative fluxes other than at the TOA exhibit substantially greater uncertainties than fluxes at the TOA, even taking into account the constraints that the net heat flux into the atmosphere be zero and into the surface be near zero. The Stefan-Boltzmann radiation law is used to calculate the longwave emission from the surface to the atmosphere, often using the global mean near-surface air temperature. Concerns over this approach are use of a global mean temperature versus more explicit consideration of spatial and temporal variation, use of the temperature of air (typically measured at 2 m) rather than that of the actual radiating element, the surface, and the usually tacit assumption that the surface emissivity is unity; for discussion see Ref. [20]. Atmospheric absorption of longwave radiation is estimated by radiative transfer calculations that take into account not only absorption by the long-lived GHGs, whose mixing ratios are more or less uniform as a function of location in the atmosphere, but also absorption by water vapor, whose mixing ratio is highly variable spatially and temporally (§IV.B), and by clouds, also

highly variable. Calculating the absorption and emission of longwave radiation by water vapor and clouds relies on representation of water vapor and cloud amount, vertical distribution, and temperature obtained from meteorological reanalyses; these reanalyses consist of weather forecast models run retrospectively, constrained by observations, using much the same physics as in climate models. Surface absorption of shortwave irradiance is estimated based on surface spectral reflectance, which is dependent on surface type, soil moisture, vegetation cover, and the like, and on the downwelling spectral irradiance incident on the surface, which is greatly influenced by the presence and nature of clouds, and thus highly variable, spatially and temporally.

Further terms in the radiation budget are transfer of latent and sensible heat from the surface to the atmosphere. Latent heat release is estimated from the precipitation rate, as the global rate of net evaporation (evaporation minus dewfall) is equal to the global rate of precipitation. The total latent heat released into the atmosphere annually, expressed per square meter of Earth surface, is equal to the amount of latent heat of condensation of water times the annual average global mean precipitation. The latent heat flux indicated in Figure 2 ($88 \pm 5 \text{ W}\cdot\text{m}^{-2}$) corresponds to an annual and global mean precipitation rate of $1.1 \pm 0.06 \text{ m}\cdot\text{yr}^{-1}$. Despite satellite-based observations, there is still substantial uncertainty in global precipitation. Recent work suggests that current estimates may be low by 10% or more.²¹ Sensible heat flux is based on model calculations that take into consideration surface wind stress (which depends on surface roughness and wind speed) and temperature gradient between atmosphere and surface, all of which quantities can be highly variable spatially and temporally; the inputs to the calculation are again obtained from meteorological reanalyses.

D. Spatial and temporal variability

At high time- and space-resolution, upwelling radiative fluxes at the TOA are much more variable than in global and longer-term means, Figure 3. The figure, which is based on essentially instantaneous measurements with satellite radiometers on two sun-synchronous polar-orbiting satellites (equator crossing, ~10:30 and ~1:45 local time) made by the NASA CERES (Clouds and the Earth's Radiant Energy System) program, illustrates the richness of the processes that govern absorption and emission of radiant energy from and to space. The local spatial structure is due largely to clouds, which are cold in the thermal infrared (because of the decrease in temperature with altitude) and bright in the shortwave. Notable is the intertropical convergence zone near the equator that is characterized by strong rising motion of the atmosphere is readily apparent in the Pacific. Contrast of bright land areas with adjacent ocean areas may be discerned, for example in northern Africa. Likewise, the contrast between hotter land surfaces and adjacent oceans is readily discerned in the thermal infrared flux at the Persian Gulf. The figure illustrates the high dynamic range of the individual upwelling radiation terms, more than $1000 \text{ W}\cdot\text{m}^{-2}$ in the shortwave and more than $300 \text{ W}\cdot\text{m}^{-2}$ in the longwave. The instantaneous net daytime flux exhibits even greater dynamic range, $\sim 1300 \text{ W}\cdot\text{m}^{-2}$. The measured fluxes must be averaged spatially and temporally and then added algebraically to determine the planetary net flux. As this net flux is confidently thought to be less than $1 \text{ W}\cdot\text{m}^{-2}$, the large dynamic ranges of the several fluxes place stringent requirements on measurement accuracy. Although the instruments aboard the Sun-synchronous satellites that are the principal sources for Earth radiation budget data are quite accurately calibrated, current satellites sample only a limited portion of the diurnal cycle. Consequently, accounting for the full diurnal cycle requires that the rest of the diurnal cycle be filled in by measurements made with less-well calibrated instruments aboard geostationary satellites. Similar accuracy is thus required from those measurements and from models used to calculate diurnal averages. The results of such

calculations are illustrated in panel *d*, which shows the smoothing that results from the summation of the several terms that is manifested in the reduced dynamic range of the data. This panel also illustrates the consequence of latitudinal transport of heat from equatorial regions (net absorption) to high latitudes (net emission).

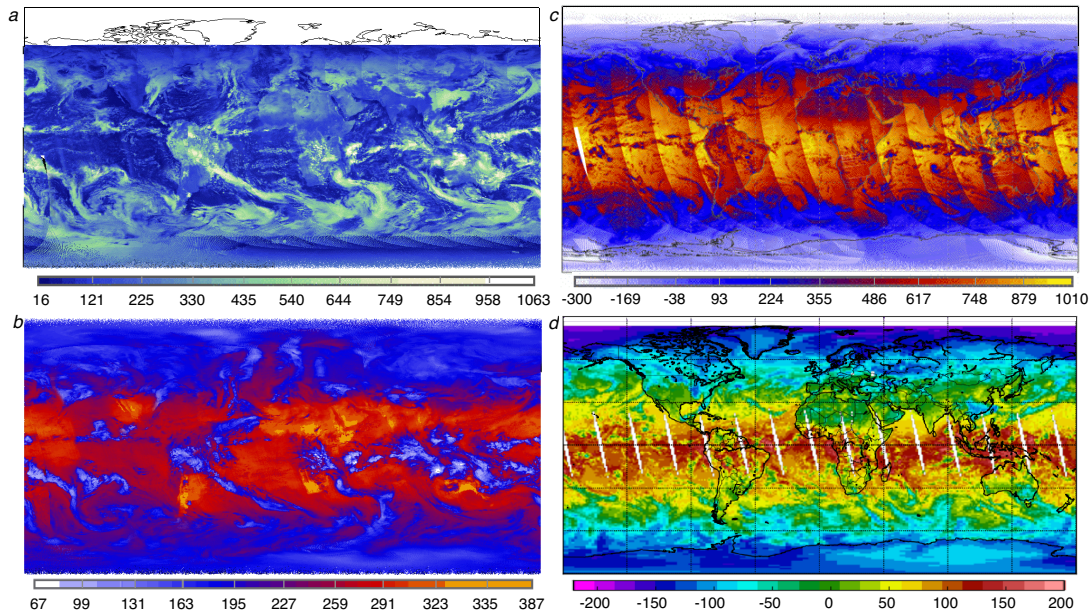


Figure 3. Local top-of-atmosphere radiative fluxes ($\text{W}\cdot\text{m}^{-2}$) as determined from satellite measurements, March 10, 2012. *a*) Instantaneous shortwave reflected flux; *b*) instantaneous longwave flux (positive upward); *c*) instantaneous net daytime flux (positive downward), evaluated as $J_S \cos \theta_0$ minus the sum of upwelling SW and LW fluxes, where J_S is the solar constant and θ_0 is the solar zenith angle; *d*) daily mean net flux (positive downward) after temporal integration. The depicted discontinuities are artifacts resulting mainly from changes, especially in cloudiness, between successive satellite overpasses. From CERES; courtesy of Norman Loeb, NASA.

A key strength of spatially resolved measurements is the ability to identify cloud-free regions and thus determine separately the irradiance from planet as a whole and from the cloud-free regions. The contribution of clouds (strictly, cloudy regions, which inevitably contain some cloud-free regions) to the short- and longwave irradiance components of the total upwelling flux, denoted cloud radiative effect, CRE, Figure 2, is determined by difference.

E. Spectral dependence

Yet another important dimension that is essential to describing Earth's energy budget is the spectral dependence of both the short- and longwave upwelling radiation. An examination of the latter, shown in Figure 4 for a single instance, is very instructive. This figure, which was obtained by an early infrared spectrometer in space,²² shows the rich spectral structure associated with the upwelling longwave radiation, specifically for a location in a moist vegetated region in the Niger valley. For this location, the radiance at the TOA is bounded by a temperature profile that corresponds to the Planck function at 320 K. In the spectral regions 8 – 9 and 10 – 12 μm , where absorption by water vapor, CO_2 , or other trace atmospheric gases is slight, the radiance at the TOA is approximately equal to that given by the Planck distribution for the surface temperature; (as the measured quantity is radiance, its numerical value is less, by roughly a factor of π , than that of irradiance given in Figure 1). These regions are denoted “window regions” of the thermal infrared. The radiation temperature in these window regions, 320 K, is a fairly accurate measure of the local emission temperature of the surface, which substantially exceeds the local surface air temperature. Attention is called to the decrease in emitted radiation in the absorption bands of the GHGs water vapor, CO_2 , ozone O_3 , and methane CH_4 , a manifestation of the greenhouse effect (§IV). These features correspond to infrared-active transitions between vibrational states of the molecules (and, for water vapor, rotational states). The radiation temperature associated with the absorption bands of the several greenhouse gases is a measure of the temperature of the atmosphere at which the gases exert their greatest influence on emission of radiation to space. The altitude z to which the temperature corresponds (by Figure 5) is down from the TOA by approximately one unit of optical depth (*i.e.*, $\int_z^\infty \sigma(z') dz' \approx 1$ where $\sigma(z')$ is the absorption coefficient of the gas at altitude, z'). The reduction

in emitted radiance due to the presence of the GHGs is about 40%. That is to say, the effective TOA emissivity relative to the Stefan-Boltzmann radiance at the surface temperature is about 60%, consistent with the value obtained above as the ratio of the upwelling global mean flux at the TOA relative to the upwelling flux calculated for the global mean surface temperature.

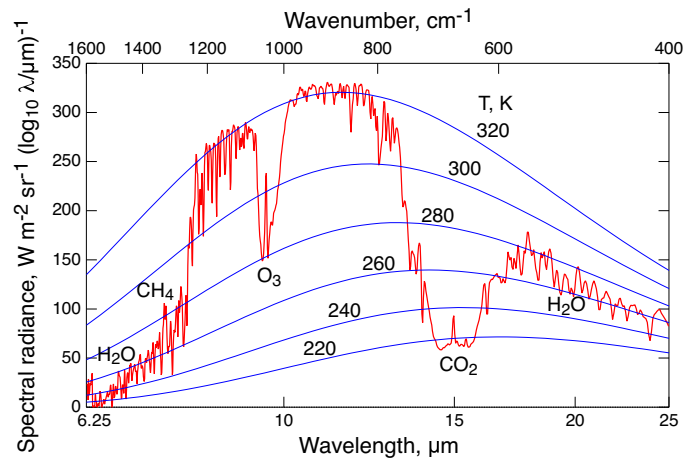


Figure 4. Dependence of upwelling thermal infrared radiance on wavelength or wavenumber (lower and upper axes, respectively, logarithmic scale) measured by interferometry from the Nimbus 4 satellite platform. Spectrum, obtained on May 5, 1970, was from a moist, vegetated area of the Niger Valley (footprint roughly 100 km 100 km, largely if not completely cloud free). Gases principally responsible for absorption are noted. Blue curves denote Planck distribution functions for indicated temperatures. Redrawn after Ref. [21]; data from ftp://acdisc.gsfc.nasa.gov/data/s4pa/Nimbus4_IRIS_Level1B/IRISN4RAD.001/1970; acknowledgment to J. E. Johnson for assistance in acquiring the data.

In contrast to the strong absorption due to the infrared-active trace gases, N_2 and O_2 , despite their much greater abundances, do not exhibit appreciable absorption in the thermal infrared, as electronic dipole vibrational transitions are strongly forbidden in homonuclear diatomic molecules because of quantum-mechanical symmetry considerations, **SN2**.

- 11.** “Über das gesetz der energieverteilung im normalspectrum,” M. Planck, *Annalen der Physik* **309**, 553-563 (1900). doi: 10.1002/andp.19013090310. English translation “On the law of distribution of energy in the normal spectrum,” <http://www.to.infn.it/~zaninett/articoli/planck.html>. Historically important. (I)
- 12.** “The Sun’s total and spectral irradiance for solar energy applications and solar radiation models,” C. A. Gueymard, *Solar energy* **76**, 423-453 (2004). Authoritative examination and tabular presentation of solar spectral irradiance. (E)-(I)
- 13.** “Planetary radiation budgets,” R. Kandel, and M. Viollier, *Space Sci. Revs.* **120**, 1-26 (2005). DOI: 10.1007/s11214-005-6482-6. Accessible introduction. (E)-(I)
- 14.** “Seasonal variation of cloud radiative forcing derived from the earth radiation budget experiment,” E. F. Harrison, P. Minnis, B. R. Barkstrom, V. Ramanathan, R. D Cess, and G. G. Gibson, *J. Geophys Res.*, **95**, 11679–11698 (1990). doi: 10.1029/JD095iD11p18687. Research paper reporting measurements from the NASA Earth Radiation Budget Experiment. (E)-(I)
- 15.** “Toward optimal closure of the Earth’s top-of-atmosphere radiation budget,” NG Loeb, BA Wielicki, DR Doelling, GL Smith, DF Keyes, S Kato, N Manalo-Smith, and T Wong *J Climate* **22**, 748-766 (2009). doi: <http://dx.doi.org/10.1175/2008JCLI2637.1>. Research paper reporting TOA fluxes determined by the NASA CERES program and associated error budget. (I)
- 16.** “A new, lower value of total solar irradiance: evidence and climate significance,” G. Kopp and J. L. Lean, *Geophys Res Lett* **38**, L01706 (2011). Research paper. (I)

17. “Joseph Fourier, the ‘greenhouse effect’, and the quest for a universal theory of terrestrial temperatures,” J. R. Fleming, *Endeavour*, 23(2), pp.72-75 (1999). Historical and pedagogical review. (E)
18. “On the Absorption and Radiation of Heat by Gaseous Matter, Second Memoir,” J. Tyndall, *Philosophical Transactions of the Royal Society of London* 152, 59-98 (1862). Historical memoir. (I)
19. “Observing and modeling Earth’s energy flows,” B. Stevens and S. E. Schwartz, *Surveys in Geophysics* 33, 779-816 (2012). Review and assessment. (I)
20. “Earth’s global energy budget,” K. E. Trenberth, J. T. Fasullo, and J. Kiehl, *Bulletin of the American Meteorological Society* 90(3), 311-323 (2009). Accessible examination of observations, models, theory. (E)-(I)
21. “An update on Earth’s energy balance in light of the latest global observations,” G. L. Stephens, J. Li, M. Wild, C. A. Clayson, N. Loeb, S. Kato, T. L’Ecuyer, P. W. Stackhouse, Jr., M. Lebstock, and T. Andrews, *Nature Geoscience* 5, 691–696 (2012). doi:10.1038/ngeo1580. Review and assessment. (I)
22. “The Nimbus 4 infrared spectroscopy experiment 1. Calibrated thermal emission spectra,” R. A. Hanel, B. J. Conrath, V. G. Kunde, C. Prabhakara, I. Revah, V. V. Salomonson, and G. Wolford, *J. Geophys. Res.*, 77(15), 2629-2641 (1972). Early infrared spectroscopic measurements from space. (E)-(I)

III. OVERVIEW OF EARTH'S CLIMATE

The physical laws governing Earth's climate are few but powerful:

- *Conservation of matter*, reflected in the continuity equation;
- *Conservation of energy*, in all its forms: radiant, kinetic, potential, sensible, and, importantly, latent heat associated with phase transitions of water;
- *Newton's second law*, represented by the Navier-Stokes equation relating the change in momentum (of parcels of air or water) to (principally) gravitational and viscous forces;
- The *Planck radiation law* for black bodies;
- *Kirchhoff's law* equating spectral absorptivity and emissivity; and
- The *ideal gas law*.

To these physical laws must be added *material properties* – thermal, spectral, the freezing point and temperature-dependent saturation vapor pressure of water, the density of liquid water and its dependence on temperature and salt concentration, surface tension of water, specific heats, viscosities, and the like – and *Earth-specific properties* such as the amount of water in the system, the salinity of the ocean, and the composition of the atmosphere. Important *boundary conditions* are the spectral irradiance of the sun, orbital geometry, Earth's diameter and rotational speed, the shapes of continents, and the elevation of the land surface and the ocean floor. Also important is the spectral reflectance of Earth's surface, importantly including biological influences. Set the system in motion and it evolves according to the several physical laws. Of course the climate system is highly nonlinear, with resultant strong sensitivity of its evolution to even slight changes in initial conditions.²³ This sensitivity limits the accuracy of any calculation of future state of the climate, necessitating solutions that are not expected to be accurate for a given date in the future but are thought to be accurate in the mean and other statistical properties. This statistical independence of initial conditions, which rests on a conjecture by Lorenz,²⁴ is widely assumed by climate scientists but is not proved and is the subject of much attention by mathematicians.²⁵

The principal constituents of the atmosphere are nitrogen, N_2 , (78%), oxygen, O_2 , (21%) and argon (1%) as mixing ratio (mole fraction) in dry air. The mixing ratio of water vapor is highly variable, from as great as 3% down to $10^{-4}\%$, as governed by temperature and relative humidity. Other gases, present in trace amounts, play no appreciable role in the physical properties of the atmosphere such as density and viscosity, but play key roles in climate because of their influences on absorption and emission of radiation.

For the purpose of this article, certain properties of Earth's present atmosphere and climate system are taken as givens, although some can be derived.^{8,10} Key among physical properties of the atmosphere is temperature structure in the lowest two major compartments of the atmosphere, which are most pertinent to climate change: the troposphere and the stratosphere, Figure 5. The troposphere is more or less well mixed by convection (vertical transport under conditions of thermally induced instability caused mainly by heating of the surface by solar radiation). The rate of decrease of temperature with altitude in the troposphere, about $6.5 \text{ K}\cdot\text{km}^{-1}$, is governed by the condition of neutral stability against vertical motion taking into account the latent heat of water condensation in addition to the heat capacity of air. The increase in temperature with increasing altitude in the stratosphere is due mostly to absorption of solar radiation, mainly by ozone; as warmer air is lighter than cooler air, the stratosphere is stable against vertical motion. The altitude of the tropopause is about 16 km in the tropics, Figure 5, decreasing poleward to about 11 km in midlatitudes and 9 km at the poles.

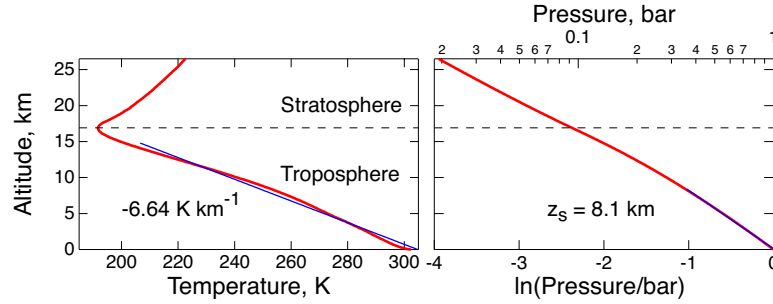


Figure 5. Vertical structure of atmospheric temperature and pressure in the lower atmosphere (by convention the independent variable altitude is shown on the y-axis). Temperature profile is annual mean at the Department of Energy Atmospheric Radiation Measurement site at Manus Island, Papua New Guinea.²⁶ Temperature decreases nearly linearly with altitude in the troposphere to a minimum at the tropopause (dashed line) above which it increases; logarithm of pressure p decreases approximately linearly with altitude. Blue lines indicate slopes of linear fits over indicated ranges; scale height is evaluated from slope as $z_s = -(d \ln p / dz)^{-1}$.

Atmospheric pressure, which is due to the gravitational force of the mass of overlying air, decreases from its value at the surface $p(0)$ nearly exponentially with altitude, z , as

$$p(z) = p(0) e^{-\frac{Mg}{R} \int_0^z \frac{1}{T(z')} dz'} \quad (6)$$

where M is the average molecular weight (molar mass) of air, $0.029 \text{ kg} \cdot \text{mol}^{-1}$, g is acceleration of gravity, $9.8 \text{ m} \cdot \text{s}^{-2}$, and R is the gas constant, $8.3 \text{ J} \cdot \text{mol}^{-1} \cdot \text{K}^{-1}$; here the ideal gas law has been employed to calculate mass concentration. The height of the atmosphere if it were compressed to sea-level pressure, 1 bar ($1 \times 10^5 \text{ Pa}$), a measure of the scale height of the atmosphere, is about 8 km . If the atmosphere were isothermal, the scale height would be equal to $RT/Mg = 8.4 \text{ km}$ for $T = 287 \text{ K}$. The troposphere and the stratosphere are more or less decoupled, as the increase in temperature with altitude in the stratosphere suppresses convective transport between the two layers. The circulation between the troposphere and the stratosphere is driven mainly by convection in the tropics and return of stratospheric air to the troposphere at high latitudes.

In addition to the climate system as a whole being in near steady state, each of its compartments is likewise in near steady state. Hence it is required that in each compartment uptake of energy via one process be balanced by loss via another process; estimates of the several energy fluxes shown in Figure 2 are constrained by this requirement. Trace atmospheric constituents play essential roles by absorption and emission of radiation in maintaining the atmospheric and surface temperature. The energy budget of the stratosphere consists of absorption of solar radiation in the ultraviolet, mainly by ozone (O_3), balanced by emission in the thermal infrared, mainly by carbon dioxide (CO_2). Although the atmosphere is highly transmissive of solar radiation, near infrared absorption contributes to the energy budget of the troposphere. Solar radiation incident on and absorbed by the surface heats the surface; the surface loses this energy mainly by radiating in the thermal infrared, as a nearly black body. Absorption of this thermal infrared energy heats the adjacent atmosphere; this heating induces convection that tends to mix the troposphere vertically. In these two ways, radiative heating is responsible to first order for the vertical structure of atmospheric temperature. Energy is lost from the atmosphere mainly by thermal infrared radiation, to the surface or to space.

Another key compartment of the climate system is the world ocean. There is much more mass in the water of the ocean than in the air in the atmosphere; the mass of an atmospheric column is equal to the mass of the top 10 m of a column of seawater. Further, the specific heat of water is several times greater than that of air. Consequently, the heat capacity of an atmospheric column is equal to the heat capacity of a column of seawater that is just 2.5-m deep. The ocean is more or less well mixed to a depth of about 100 m, roughly the depth of penetration of the seasonal variation of air temperature. The atmosphere rapidly exchanges heat with the upper ocean, on a time scale less than a year; the exchange of heat between the upper ocean and the deep ocean is

much slower than mixing in the upper ocean. Based on these considerations the effective heat capacity of the climate system, at least on the time scale of a decade or so, is that of the top 100 - 200 m of the ocean, whereas on longer time scales the rate of climate change is governed by the rate of transfer of heat to the deep ocean. The world ocean thus serves as the flywheel of the climate system, tending to damp rapid fluctuations in the temperature of the atmosphere. Finally, in contrast, change in heat content of land is much less important because of the lower specific heat and lower rate of heat transfer in solid earth.

23. “Deterministic nonperiodic flow,” E. N. Lorenz, *J. Atmos. Sci.* **20**, 130-141 (1963).

Historically important paper on chaos in atmospheric science. (A)

24. “Predictability; Does the flap of a butterfly’s wings in Brazil set off a tornado in Texas?” E. N. Lorenz, American Association for Advancement of Science, Talk presented Dec. 29, Section on Environmental Sciences, New Approaches to Global Weather: GARP. Boston, MA (1972). http://web.mit.edu/lorenzcenter/about/LorenzPubs/Butterfly_1972.pdf.

Historically important and accessible. (E)

25. “The Lorenz Attractor, A Paradigm for Chaos,” É. Ghys, in **Chaos** (pp. 1-54), Editors: B. Duplantier, S. Nonnenmacher, and V. Rivasseau (Springer Basel, 2013). Mathematical.

(A)

26. “Response of tropical precipitation to global warming,” D. M. Romps, *J. Atmos. Sci.* **68**, 123-138 (2011). Cited as providing vertical temperature profiles. (I)

IV. THE GREENHOUSE EFFECT

A. Role of the greenhouse effect

As noted in §I, the greenhouse effect is central to the climate system of Earth (and also of Mars and Venus²⁷). Radiative effects of GHGs play a central role in climate change because of the increase in the greenhouse effect resulting from increases in amounts of atmospheric GHGs over the Anthropocene. It is thus essential to understand the greenhouse effect and its dependence on properties of the atmosphere. From **SN3** it is seen that the greenhouse effect induced by infrared-active gases consists of three elements:

- Downwelling longwave irradiance from the atmosphere to the surface, heating the surface and elevating the surface temperature;
- A decrease in upwelling irradiance at the TOA; and
- Radiative cooling and heating of the atmosphere, affecting the vertical temperature structure of the atmosphere.

All of these phenomena depend on absorbance and its wavelength dependence, on temperature, and on the vertical distributions of these quantities. The TOA greenhouse effect consists of two terms: absorption which results in a decrease in outgoing longwave radiation; and emission, which results in an increase that is subtractive from the first term; the two terms are comparable in magnitude, but the absorption term dominates. The distribution between the two terms depends on the energy of the transition. These effects are examined quantitatively in **SN4**.

B. Greenhouse gases in Earth's atmosphere

It is important to distinguish the GHGs in Earth's atmosphere that might be considered external to the climate system from water vapor, which must be considered an intrinsic component of the climate system, as the amount and distribution of water vapor are controlled by meteorological

processes. Water in the atmosphere is present primarily as vapor; even in clouds, the amount of vapor typically exceeds the amount in the condensed phase by one or two orders of magnitude. A control on the amount of water vapor in the atmosphere is the local temperature, which, through the Clausius-Clapeyron equation, sets an effective upper limit to the water vapor partial pressure. Over the global range of surface temperatures, -40 to $+35$ °C, the equilibrium partial pressure of water vapor varies by a factor of 400, and when the range is extended to tropopause temperature, 210 K, a further factor of 20.

The sources of atmospheric water vapor, evaporation of liquid water (and sublimation of ice) and transpiration through the leaves of vegetation, are highly variable in space and time. The rate of evaporation of water from liquid surfaces and moist soil depends strongly on temperature, relative humidity, wind speed, and local turbulence. The rate of transpiration is affected also by sunlight intensity and by water stress, which induces stomatal closure in plants.²⁸ The principal process whereby water is removed from the atmosphere is precipitation, which is intermittent, with condensation (dew, frost) a distant but non-negligible second. The release of latent heat as water vapor condenses warms the air, enhancing buoyant convection, and thus plays a large role in the dynamics and vertical transport of the atmosphere. Conversely, as air is warmed by compression during downward motion, evaporation of water cools the air, enhancing the downward motion or suppressing convection. Water vapor is short-lived in the atmosphere compared to other major GHGs. Estimating the mean atmospheric residence time of water vapor as the amount of water in the atmosphere divided by the precipitation rate yields for typical column amount of water vapor equivalent to 2.5 cm of liquid water and precipitation rate $1 \text{ m}\cdot\text{yr}^{-1}$ a mean residence time of 0.025 yr, or 9 days. Such a short residence time, together with the spatial variability of sources and temporal intermittency of removal processes, contributes

further to the large spatial and temporal variability of water vapor in the troposphere, Figure 6.

For these reasons, it is useful to consider water part of the climate system.

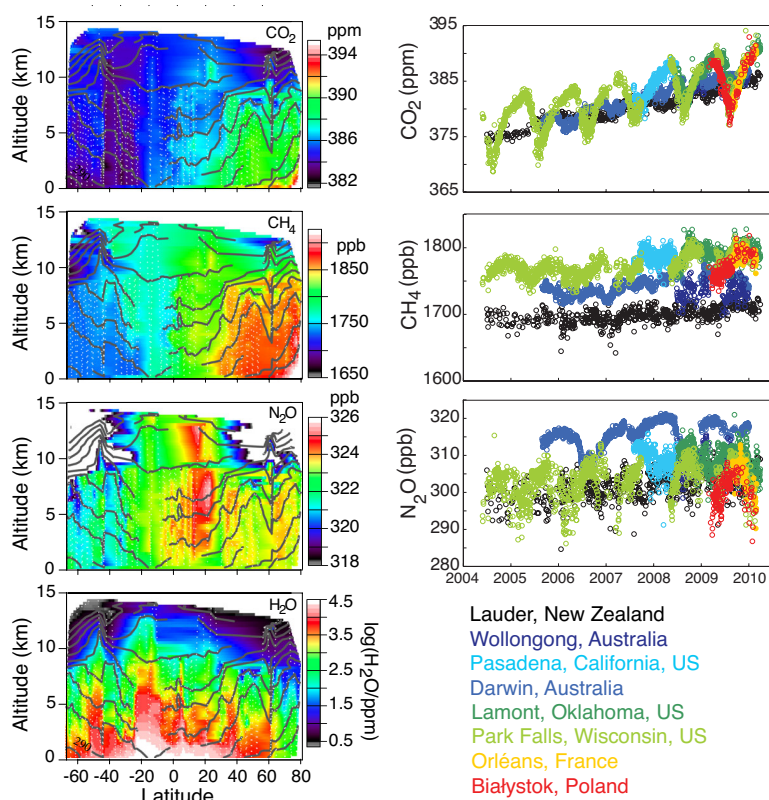


Figure 6. Space and time variation in atmospheric greenhouse gases in the troposphere and lower stratosphere. *Left*, Mixing ratios of CO_2 , CH_4 , and N_2O , and water vapor (log scale) along the date line, January 2009. Modified from Ref. [29]. *Right*, Time series of daily-median column-averaged mixing ratios of CO_2 , CH_4 and N_2O at several sites. Modified from Ref. [30]. Mixing ratio, denotes mole fraction relative to dry air, generally expressed as ppm (parts per million) or ppb (parts per billion).

In addition to water vapor, the principal greenhouse gases in Earth's atmosphere are carbon dioxide (CO_2), methane (CH_4), nitrous oxide (N_2O), and chlorofluorocarbons (CCl_2F_2 , CCl_3F), all of which are long-lived in the atmosphere (decade to century). Such lifetimes are much greater than the time required for a gas to become well mixed within the atmosphere (~ 3 weeks in a given latitude band, ~ 3 months hemispherically, 1-2 years globally). Hence, these gases are quite uniformly distributed in the atmosphere, with variations typically 10% or less, Figure 6.

CO₂ exhibits seasonal variation due to seasonal uptake and release by terrestrial vegetation; this seasonal variation is greater in the Northern Hemisphere than the Southern Hemisphere because of greater land mass. Locally, near emission sources or in poorly ventilated vegetated canopies, CO₂ can exhibit considerably greater variation. Importantly, as discussed in §V, the amounts of these gases in the atmosphere have increased substantially over the Anthropocene; these increases are the basis for concern over the human-induced increase in the greenhouse effect. Changes in the atmospheric mixing ratios of these long-lived GHGs are usefully considered controlled by processes external to the climate system.

The radiative effects of GHGs, including water vapor, can be calculated using models of varying complexity, depending on application.²⁷ The most detailed models explicitly represent infrared transitions on a line-by-line basis that includes representation of altitude dependence of collisionally induced broadening (SN4) and representation of the water vapor continuum. The mixing ratios of the several GHGs and the vertical structure of temperature and water vapor are the inputs to the model calculations. These models have been extensively evaluated under conditions for which the atmospheric structure of temperature and water vapor is accurately and independently measured. Departures of modeled and observed downwelling clear-sky fluxes, over a wide range of atmospheric states, are less than $1.5 \text{ W}\cdot\text{m}^{-2}$.³¹ With confidence in the line-by-line models, they can serve as the basis for formulating less spectrally resolved rapid radiation transfer models that can be employed for calculating radiative effects of GHGs in climate models.^{32,33}

27. “Infrared radiation and planetary temperature,” R. T. Pierrehumbert, *Physics Today* 64(1), 33-38 (2011). Lucid blend of observation and theory. (E)

- 28.** “Measuring H₂O and CO₂ fluxes at field scales with scintillometry: Part II—Validation and application of 1-min flux estimates,” B. Van Kesteren, O. K. Hartogensis, D. van Dinter, A. F. Moene, and H. A. R. De Bruin *Agric. For. Meteorol.*, **178**, 88–105 (2013). (I)
- 29.** “HIAPER Pole-to-Pole Observations (HIPPO): Fine-grained, global-scale measurements of climatically important atmospheric gases and aerosols,” S. C. Wofsy and The HIPPO science team and cooperating modellers and satellite teams. *Philosophical Transactions of the Royal Society A: Mathematical, Physical and Engineering Sciences*, **369**, 2073-2086 (2011). (E)
- 30.** “The total carbon column observing network,” D. Wunch, G. C. Toon, J. F. L. Blavier, R. A. Washenfelder, J. Notholt, B. J. Connor, D. W. T. Griffith, V. Sherlock, and P. O. Wennberg, *Philosophical Transactions of the Royal Society A: Mathematical, Physical and Engineering Sciences* **369**, 2087-2112 (2011). (E)
- 31.** “The QME AERI LBLRTM: A closure experiment for downwelling high spectral resolution infrared radiance.” David D. Turner, D. C. Tobin, Shephard A. Clough, Patrick D. Brown, Robert G. Ellingson, Eli J. Mlawer, Robert O. Knuteson, et al, *J. Atmos. Sci.* **61**, 2657-2675 (2004). (I)
- 32.** “Atmospheric radiative transfer modeling: A summary of the AER codes,” S. A. Clough, M. W. Shephard, E. J. Mlawer, J. S. Delamere, M. J. Iacono, K. Cady-Pereira, S. Boukabara, and P. D. Brown, *Journal of Quantitative Spectroscopy and Radiative Transfer* **91**, no. 2 (2005): 233-244. (A)

33. “Radiative forcing by long-lived greenhouse gases: Calculations with the AER radiative transfer models,” M. J. Iacono, J. S. Delamere, E. J. Mlawer, M. W. Shephard, S. A. Clough, and W. D. Collins *J. Geophys. Res.* 113, D13103 (2008). doi:10.1029/2008JD009944. This and the two previous references are examples of state-of-the-art modeling of atmospheric radiation transfer. (A)

V. RADIATIVE FORCING OF CLIMATE CHANGE

The key questions that face the climate change research community today deal with anthropogenic influences on the planetary radiation budget and responses of the climate system to perturbations. As is well established by measurements, atmospheric mixing ratios of several long-lived gases that contribute to Earth’s greenhouse effect have increased substantially over the past 250 years because of human activities, Figure 7. Mixing ratios prior to contemporary measurements are from glacial ice cores, mainly in Antarctica, for which the record extends to 800,000 years before the present. The dataset initiated in 1958 by Charles David Keeling at Mauna Loa, Hawaii, isolated from local sources and sinks and thus representative of the Northern Hemisphere, reveals the annual cycle of draw down and release of CO₂ by terrestrial vegetation. This dataset has become an icon of the anthropogenic influence on GHG concentrations. The increase in abundance of carbon dioxide and methane over the Anthropocene is comparable to the increase between the last glacial maximum and the Holocene. Shown on the right hand axes of the several panels in Figure 7, are the perturbations in the longwave radiation budget of the planet that would result from the increases in the mixing ratios of the several gases. This hypothetical increase in the net rate of uptake of energy by the climate system (or more generally, any such change in Earth’s energy budget that is imposed from outside the climate system), is denoted a *forcing*; like the energy fluxes themselves, forcings are commonly given

normalized to the area of the planet, with unit $\text{W}\cdot\text{m}^{-2}$. The sum of the several forcings, imposed over the Anthropocene because of the increase in abundance of GHGs over this period, leads to expectation of a resultant increase in the greenhouse effect and consequent increase in Earth's surface temperature. The increases in atmospheric abundances of the so-called long-lived GHGs, most importantly carbon dioxide (CO_2), but also including methane (CH_4), nitrous oxide (N_2O), and chlorofluorocarbons (CCl_2F_2 , CCl_3F) are at the core of the present concern over anthropogenic global warming, or more broadly over anthropogenic climate change.

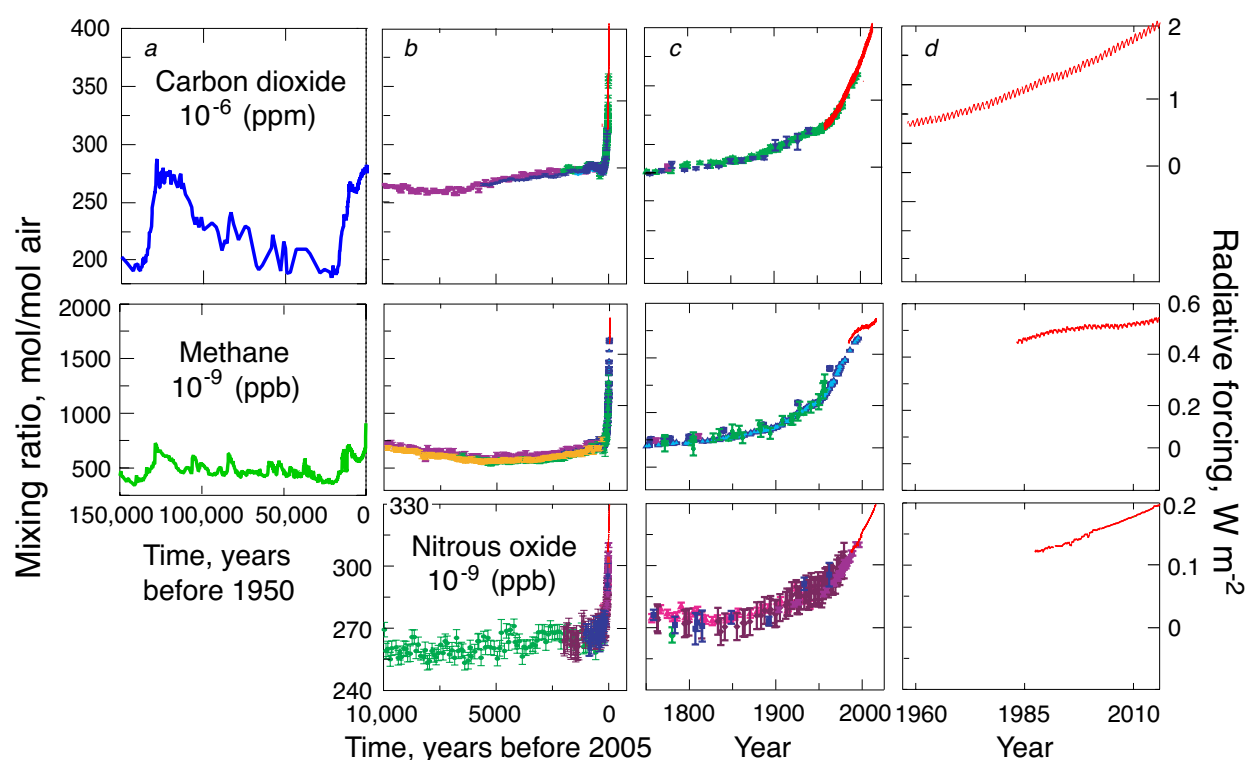


Figure 7. Atmospheric mixing ratios (left axes) and resulting global-mean perturbations in radiative budget (radiative forcings, right axes) of carbon dioxide, methane, and nitrous oxide over *a*, the last glacial-interglacial cycle, 150,000 years; *b*, the Holocene, 10,000 years; *c*, the Anthropocene, 250 years, and *d*, contemporary measurements at Mauna Loa, Hawaii. Measurements from Antarctic ice cores in *b* and *c* are shown as symbols with different colors for different studies; contemporaneous atmospheric measurements are shown by red curves. *a*, CO_2 , Ref. [34]; CH_4 , Ref. [35]; *b*, *c*, modified from the Fourth IPCC Assessment Report (Ref. [5] §6.4.1.1); *d*, monthly mean data from NOAA (ftp://aftp.cmdl.noaa.gov/data/trace_gases/) and, for CO_2 , Scripps Institution of Oceanography http://scrippsco2.ucsd.edu/research/atmospheric_co2, updated from Ref. [36].

The magnitude of forcing by the several long lived GHGs, about $3 \text{ W}\cdot\text{m}^{-2}$ at present relative to the preindustrial atmosphere, is some two orders of magnitude less than the global and annual mean outgoing longwave flux at the TOA or than the corresponding average downwelling or upwelling longwave fluxes at the surface (Figure 2). This disparity serves to justify treating this forcing as a perturbation on the climate system. Moreover, the spatial and temporal variations in the several fluxes inherent in the climate system (Figure 3) greatly exceed the magnitude of the perturbation due to increased amounts of atmospheric GHGs, challenging the capability to measure the radiative effects of the incremental GHGs. Consequently, these radiative effects are determined by calculation, based on the absorption spectra of the several gases and the atmospheric state.

In parallel with the increases in atmospheric amounts of GHGs over the Anthropocene, industrial activities have resulted in increases in the amounts of aerosols in the troposphere. Aerosol particles scatter shortwave radiation and increase the reflectivity and persistence of clouds; increases in aerosol loadings would be thus expected to reduce the absorption of shortwave radiation incident on the planet, thereby changing Earth's radiation budget (i.e., exerting a forcing) in a direction opposite to the increase in net energy due to increased GHGs. The magnitudes of the radiative perturbations due to anthropogenic aerosols are confidently thought to be comparable to those of the GHGs, but the perturbations are much less well understood and quantified; absorption of shortwave radiation by soot particles lends further complexity to the aerosol forcing. Incremental tropospheric aerosols are produced largely as a consequence of fossil fuel combustion through direct emission and atmospheric reactions involving sulfur and nitrogen oxides emitted as combustion byproducts. A major difference between the influences of incremental GHGs and incremental aerosols arises from the vast difference in atmospheric

residence times of the GHGs (decades to centuries) and the tropospheric aerosols (about 10 days, through removal mainly by precipitation), the implications of which are examined in §VIII. Quantitative understanding of the climate system response to perturbations over the Anthropocene and to responses to future changes in atmospheric composition must take all of these perturbations into account. As the aerosol influences are not well understood, they are the subject of much current research.³⁷ Present best estimates by the IPCC⁴ of global-mean forcings of Earth's radiation budget over the Anthropocene epoch are shown in Figure 8. The sign convention is that forcings, which increase the net energy of the planet, are denoted as positive and those which decrease the net energy are negative; thus forcings by incremental GHGs are positive and forcings by incremental aerosols are (in the aggregate) negative. As discussed in §VII and **SN7**, change in GMST in response to forcings can be considered in good approximation to be linear, at least to first order; that is for a forcing of a given type the response is proportional to the strength of the forcing, and forcings of different types are algebraically additive. Thus, the negative forcing by anthropogenic aerosols must be considered as offsetting some fraction of the positive forcing by GHGs.

In addition to the gradual, longer-term perturbations due to the build up of atmospheric GHGs and aerosols over the Anthropocene, the total forcing has been punctuated by intermittent large negative forcings arising from major volcanic eruptions. These eruptions inject sulfur dioxide into the stratosphere; sulfuric acid aerosol formed from this sulfur dioxide scatters incident shortwave radiation, and increasing the planetary albedo. The forcing from a given volcanic eruption decreases gradually over a several-year period as the aerosol is removed from the stratosphere as stratospheric air is exchanged with that of the troposphere; once in the

troposphere the aerosol is rapidly (weeks) removed from the atmosphere, mainly by precipitation.

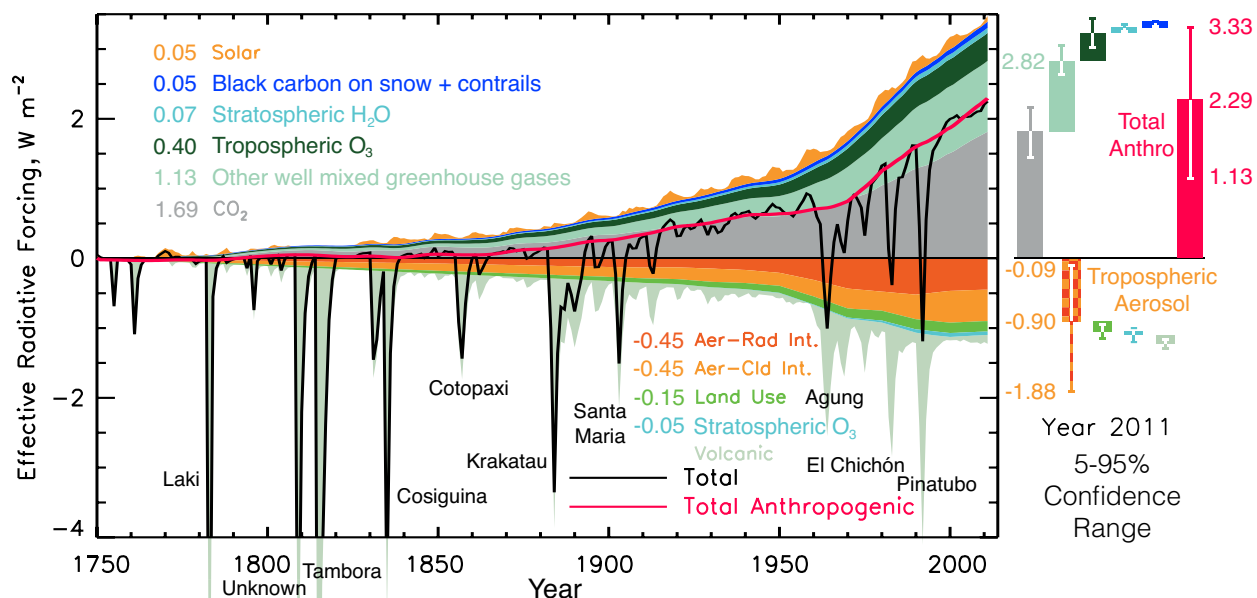


Figure 8. Radiative forcings, relative to 1750, by key climate influencing agents over the Anthropocene epoch, *left*, and for 2011, numerical values and bars at *right*. Bar denoting forcing by tropospheric aerosols represents the sum of direct aerosol interaction with radiation (Aer-Rad Int.) and indirect interaction through aerosol cloud interactions (Aer-Cld Int.). Uncertainties on bars represent central 90% range of likelihood distribution. Large negative spikes denote forcing by aerosols, mainly in the stratosphere, resulting from major volcanic eruptions; magnitudes of early volcanos are truncated. Modified from IPCC⁴, Figure 8.18 by addition of numerical values from Table 8.6 and of names of major volcanos.

Shown at the right of Figure 8 are the best estimates of the values of present (2011) forcings by the several forcing agents (bars) and of the associated uncertainties (I-beams denoting central 90% of likelihood distribution) given by the 2013 IPCC assessment⁴. The relatively small uncertainties associated with forcings by the incremental GHGs contrast to the quite large uncertainties associated with the incremental tropospheric aerosols reflected in the large uncertainty range given in the Assessment [-0.09 – -1.88 W·m⁻²]. As a consequence of the additivity of forcings, the best estimate of total forcing carries with it the uncertainty associated

with the aerosol forcing. If the aerosol forcing is at the low-magnitude end of the indicated range, then the aerosol is offsetting only a small fraction of the forcing by GHGs, and the total forcing is at the high end of the indicated range, $3.33 \text{ W}\cdot\text{m}^{-2}$. If, however, the aerosol forcing is at the high-magnitude end of the uncertainty range, the offset of GHG forcing by aerosol forcing is quite substantial, with the total forcing $1.13 \text{ W}\cdot\text{m}^{-2}$. The resultant uncertainty in total forcing is thus a factor of 3. As discussed in §VII this uncertainty in total forcing over the Anthropocene epoch, has major implications with respect to interpretation of climate change over this period.

34. “High-resolution carbon dioxide concentration record, 650 000–800 000 years before present,” D. Lüthi, M. Le Floch, B. Bereiter, T. Blunier, J.-M. Barnola, U. Siegenthaler, D. Raynaud, J. Jouzel, H. Fischer, K. Kawamura, and T. F. Stocker, *Nature* **453**, 379–382 (2008). doi:10.1038/nature06949. (E)

35. “Orbital and millennial-scale features of atmospheric CH₄ over the past 800 000 years,” L. Loulergue, A. Schilt, R. Spahni, V. Masson-Delmotte, T. Blunier, B. Lemieux, J.-M. Barnola, D. Raynaud, T. F. Stocker, and J. Chappellaz, *Nature* **453**, 383–386 (2008). doi:10.1038/nature06950. (E)

36. “Interannual extremes in the rate of rise of atmospheric carbon dioxide since 1980,” C. D. Keeling, T. P. Whorf, M. Wahlen, and J. V. D. Plicht, *Nature* **375**(6533), 666–670 (1995). A key research paper by one of the most important figures in the field. (I)

37. “Aerosol properties and processes: A path from field and laboratory measurements to global climate models,” S. J. Ghan, and S. E. Schwartz, *Bull. Amer. Meteorol. Soc.* **88**, 1059–1083 (2007). Review of processes controlling amount and properties of atmospheric aerosols. (E)-(I)

VI. THE INTENSIFIED GREENHOUSE EFFECT

The foregoing overview of the climate system, with emphasis on the processes that control Earth's radiation budget, permits examination of the anthropogenic perturbations to this budget. The important drivers of this change are increases in atmospheric infrared-active gases over the Anthropocene, some of which are shown in Figure 7, and increases in tropospheric aerosols. This section examines the changes in amounts of greenhouse gases and the resultant forcings. Determination of the changes in Earth's radiation budget due to perturbations in composition requires knowledge of the increments in atmospheric abundances of the pertinent substances and evaluation of the resulting perturbations in radiation. The forcings by incremental greenhouse gases are, to a good approximation, linear in the amount of incremental gas. It is thus possible to separate the calculation of the forcing into two components: 1) determination of the anthropogenic perturbation to the amount of greenhouse gas, and 2) determination of the change in TOA flux per increment of the gas. This separation simplifies the problem and permits attribution of the sources of uncertainty to one or the other component.

A. Anthropogenic increments in greenhouse gases

As shown in Figure 7, the amounts of carbon dioxide, methane, and nitrous oxide, which had been relatively constant for several thousand years, have increased substantially and systematically over the past two centuries, a consequence of human activities. These increments are firmly established by measurements in ice cores and, for more recent times, direct atmospheric measurements. The increase in the amount of CO₂ in the first half of the 19th century was due mainly to deforestation;³⁸ subsequently this increase has been increasingly dominated by emission from fossil fuel combustion, which now accounts for about 80% of total emissions. The

increases in methane and nitrous oxide are due to a mix of energy production activities and agriculture and animal husbandry. Additionally, industrially produced chlorofluorocarbons CCl_2F_2 and CCl_3F , which are also strongly infrared-active, have been inadvertently introduced into the atmosphere as a consequence of their use as refrigerants and propellants. Although production of these gases has been greatly curtailed because of their role in depletion of stratospheric ozone, these gases remain present in the atmosphere. These changes in atmospheric composition have resulted in a change Earth's radiation budget, mainly in the longwave, and thus a radiative forcing of climate change.

B. Radiative forcing by incremental greenhouse gases

The radiative forcing due to an increase in the amount of a greenhouse gas in the atmosphere is the net decrease in outgoing longwave radiation at the TOA that would result from such an increase prior to any increase in Earth's surface temperature that would counteract the radiative imbalance imposed by this increase. This forcing is determined by radiation transfer calculations that rely on the spectroscopic properties of the several gases. Such radiation transfer calculations are carried out with global-scale models that have realistic distributions of temperature, clouds, and water vapor. Integration over space and over an annual cycle (or perhaps several years to average out fluctuations) yields the forcing for a given increment of greenhouse gas or gases. The example calculation of radiative forcing in **SN4** explicitly illustrates the dependence of this forcing on the vertical temperature structure of the atmosphere.

Calculations such as those in **SN4**, but carried out globally and over annual and diurnal cycles, have led to development of simplified expressions for the global mean forcings of the several long lived GHGs given in Table 1. The dependence of CO_2 forcing on mixing ratio shown in the

table as logarithmic is sublinear in mixing ratio (slope decreases with increasing value of argument), as the increase in absorption is due only to increased absorption in the wings of the lines, the line centers being saturated. For CH_4 and N_2O the lines are not quite so saturated, resulting in an increase in forcing with increasing mixing ratio that is less sublinear than that of CO_2 and which is commonly represented as a square-root dependence. For the chlorofluorocarbons CCl_2F_2 and CCl_3F , which are entirely anthropogenic and for which the base-case mixing ratio is zero, the forcing is linear in mixing ratio and is much stronger per incremental mixing ratio than for CO_2 . Although commonly given expressions for forcing by the incremental GHGs are sublinear, the forcings to date, relative to the preindustrial climate, are approximately linear, Figure 9, although sublinear expressions would be needed for wider ranges of mixing ratios. The linearized expressions given in Table 1 explicitly show the much stronger forcing per increment of mixing ratio for chlorofluorocarbons, followed by N_2O and CH_4 than for CO_2 . It is this variation in forcing per incremental amount of gas in atmosphere, which gets entirely obscured by the several different functional forms, that is much more the take-home message than any nonlinear dependence on mixing ratio.

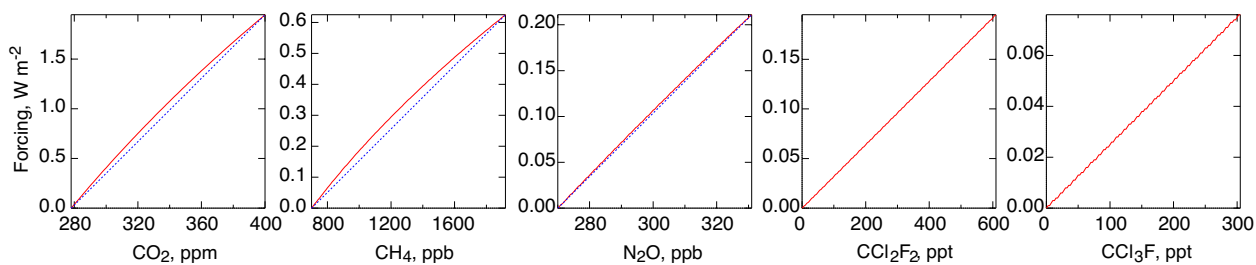


Figure 9. Global average radiative forcing by long-lived greenhouse gases as a function of their mixing ratios (parts per million, ppm; billion, ppb; trillion, ppt) shown on abscissa beginning at preindustrial values and extending approximately to present values. Red, forcing calculated by approximate formulas.³⁹ Blue lines denote linear dependence of forcing on mixing ratio. Note differences in horizontal and vertical scales for the several gases.

Trace Gas	Preindustrial mixing ratio, x_0 , ppb	2012 mixing ratio, x , ppb	Expression for forcing, $W \cdot m^{-2}$	2012 forcing $W \cdot m^{-2}$	Slope of linear fit, $W \cdot m^{-2} \cdot ppb^{-1}$	Adjustment time yr
CO ₂	278×10^3	393×10^3	$5.35(\ln x - \ln x_0)$	1.84	0.0000159	45*
CH ₄	700	1815	$0.036(\sqrt{x} - \sqrt{x_0})$	0.51	0.00051	12
N ₂ O	270	325	$0.12(\sqrt{x} - \sqrt{x_0})$	0.18	0.0035	120
CCl ₂ F ₂	0	550	$0.33(x - x_0)$	0.17	0.33	100
CCl ₃ F	0	235	$0.25(x - x_0)$	0.06	0.25	45

*Adjustment time for CO₂ would be expected to increase on time scale of centuries.

Table 1. Mixing ratios, forcings, and adjustment times of long-lived greenhouse gases; forcings are at the tropopause, not top of atmosphere. Mixing ratio x is in parts per billion, ppb; subscript 0 denotes preindustrial. Expressions for forcings from Ref. [39]. Linear approximations are shown in Figure 9. Mixing ratios and forcings are from NOAA annual greenhouse gas index <http://www.esrl.noaa.gov/gmd/aggi/aggi.html>; accessed 2013-08-17. Adjustment times from IPCC (Ref. [4]; §8.3) except for CO₂.

Because of the importance of forcing by GHGs as a driver of climate change, and because forcing cannot be directly measured (SN5) but can be determined only by radiative transfer calculations, such calculations assume considerable significance. A measure of the accuracy of such calculations comes from comparisons of forcings as calculated by multiple models. The global mean forcing that would result from doubling the atmospheric mixing ratio of CO₂, as calculated for a cloud-free atmosphere by several radiation transfer models and by the radiation codes of several general circulation climate models, was found to exhibit quite small spread (standard deviation $0.07 W \cdot m^{-2}$ or 1.6%). This small spread is indicative of the confidence that can be placed in such calculations.⁴⁰ However, as the comparison was conducted for a cloud-free planet in order to avoid complications arising from differing treatments of clouds in climate models, the resulting forcing, about $4.5 W \cdot m^{-2}$, substantially exceeds the $3.7 W \cdot m^{-2}$ for forcing by doubled CO₂ obtained with the widely used expression in Table 1. Moreover, it has become appreciated in the past several years that the introduction of a greenhouse gas into the

atmosphere would likely induce changes in atmospheric thermal structure and in turn clouds, thereby modifying the radiative impact of the incremental greenhouse gas from what it would be with static atmospheric structure. As this adjustment occurs rapidly (days to weeks), well prior to appreciable response of global surface temperature to the forcing,^{41,42} the resultant radiative changes are more usefully viewed as altering the forcing rather than as a response of the climate system to the forcing. The resulting forcing has been denoted the “adjusted forcing.” The inter-model spread in adjusted forcing by doubled CO₂ is much greater than that obtained for the pure radiative forcing in the absence of clouds and without accounting for adjustments. For the 23 climate models that participated in the 2013 IPCC model comparisons the adjusted forcing exhibited a mean of 3.44 W·m⁻², and 90% uncertainty range [± 0.84 W·m⁻²], equivalent to [$\pm 24\%$]. This spread in estimated forcing is close to the IPCC⁴ estimate of 90% uncertainty range in forcing by long-lived GHGs, [$\pm 20\%$]. Of course, the question always remains whether spread in model calculations is an accurate estimate of uncertainty, but it is in some sense a lower bound to the uncertainty that can be ascribed to present estimates.

One further greenhouse gas that should be mentioned is tropospheric ozone, which is produced by atmospheric chemical reactions involving nitrogen oxides emitted as byproducts of fossil fuel combustion and natural and anthropogenic hydrocarbons. Concentrations of ozone have increased substantially over the past 250 years. As production is localized to areas of high emission density and exhibits a rather strong seasonal cycle, and as excess atmospheric ozone is rather short lived (months), the gas is rather nonuniformly distributed spatially and temporally. The best estimate of the greenhouse forcing by incremental tropospheric ozone is about 0.4 ± 0.2 W·m⁻²; a forcing of this magnitude, although not negligible as an agent of climate change, is fairly small relative to forcing by the incremental long-lived GHGs. The large relative

uncertainty, [$\pm 50\%$] (central 90% of the likelihood distribution), is due much more to uncertainty in the amount and distribution of the increase in tropospheric ozone over the Anthropocene than to uncertainties associated with radiative transfer.

In summary, current estimates of radiative forcing by incremental GHGs, at present and as a function of time over the Anthropocene, rest on radiative transfer calculations, averaged globally and over the annual cycle. They take into account the optical properties of the gases and other controlling influences, importantly temperature and its vertical structure, spectral interference by other GHGs including water vapor, and interference by clouds (*e.g.*, Ref. [43]). Although based on well-understood physics, such calculations are not trivial. Temperature exhibits seasonal and more rapid variation, affecting greenhouse gas forcing directly and indirectly through radiative interactions with water vapor and clouds. Consequently, even though the incremental amount of the gas is fairly uniformly distributed in the global atmosphere on account of the long residence times of these gases, forcings by incremental GHGs are, in general, dependent on location, season, time of day, etc. All of these situational dependences must be accounted for in calculating the global averages of the several forcings. Still more complicated is modeling of forcings by tropospheric aerosols, whose properties and distributions in the atmosphere are highly nonuniform and whose interactions with clouds are not yet well understood. It is estimates of forcings obtained in this way, together with uncertainties inferred from inter-model spread and observational constraints, that were examined in the 2013 IPCC Assessment⁴ and which are summarized in Figure 8.

Two more important points should be noted regarding forcings. First, as indicated in §V and examined further in §VII, the forcing by increases in GHGs over the Anthropocene represents the amount by which the longwave energy leaving the planet would have decreased, relative to

the preindustrial steady state, in the absence of any increase in global temperature and resultant change in longwave emission (and/or shortwave absorption) that would offset that imbalance. As discussed in **SN1**, a forcing of $3 \text{ W}\cdot\text{m}^{-2}$ if not compensated by restoration of the planetary energy balance resulting from increase in surface temperature, would result in a planetary warming rate much greater than has been experienced over the Anthropocene. Thus the change in net irradiance at the TOA in response to this applied forcing (i.e., the planetary energy imbalance) must be well less than the applied forcing, and this would apply in general for the planetary response to any applied forcing.

A second important point about the forcing by increases in GHGs over the Anthropocene is that this forcing represents a perturbation of about 1% of the total global and annual mean outgoing longwave radiation at the TOA. The requirement is thus to determine the consequences of a 1% change in a quantity that is highly variable spatially and temporally to some desired accuracy, say 25%. This is a key reason why quantifying the effects of the increases in GHGs on Earth's climate has been and continues to be such a challenge.

C. Adjustment times of forcing agents

A further important property of forcing agents (greenhouse gases, aerosols) influencing their impacts on climate change is their residence times in the atmosphere. These residence times are governed by chemical, physical, and, for CO_2 , biological processes that remove the substances from the atmosphere. Removal of greenhouse gases methane, nitrous oxide, and chlorofluorocarbons takes place largely by gas-phase chemical reactions on time scales of a decade or so (CH_4) to a century or so (N_2O , CFCs), Table 1. Aerosol particles are removed from the atmosphere mainly by precipitation and, especially for larger particles (diameter $\geq 3 \mu\text{m}$)

gravitationally and/or and inertially induced deposition to the surface, on a much shorter time scale, about a week. The situation with anthropogenic CO₂ is more complicated, because of the abundant natural background of CO₂ with sources and sinks that greatly exceed the source strength of anthropogenic CO₂. It is thus necessary to distinguish the mean atmospheric residence time of CO₂, from what is termed the *adjustment time* of incremental CO₂, the time constant that would characterize the rate of removal of incremental CO₂ in the atmosphere relative to the preindustrial amount (*e.g.*, Ref. [4], Glossary, p. 1457). This adjustment time is the quantity that characterizes the persistence of the intensified greenhouse effect of anthropogenic emissions of CO₂. The role of natural sources and sinks of CO₂ is manifested in the annual fluctuations of atmospheric CO₂ mixing ratio seen, for example, in the Mauna Loa record, Figure 7. From estimates of the rate of uptake of CO₂ into the terrestrial biosphere and ocean (Ref. [5], Figure 7.3) the mean residence time of atmospheric CO₂ (amount in the atmosphere divided by removal rate) is estimated at about 3 yr. However, the residence time reckoned in this way is inappropriate for consideration of the adjustment time of incremental CO₂. From its definition, it is seen that the adjustment time of incremental CO₂ is a hypothetical quantity, as it cannot be directly measured. However, it can be inferred by modeling⁴⁴ or from considerations of the budget of excess atmospheric CO₂, SN6. Budget considerations indicate an adjustment time for CO₂ at present of about 45 years, increasing somewhat from 1958 to the present and thus likely to continue to increase in the future.

38. “A three-dimensional model of atmospheric CO₂ transport based on observed winds: 1. Analysis of observational data,” C.D. Keeling, R.B. Bacastow, A.F. Carter, S.C. Piper, T.P. Whorf, M. Heimann, W.G. Mook, and H. Roeloffzen, in D.H. Peterson (editor), **Aspects of Climate Variability in the Pacific and the Western Americas**, Geophysical Monograph

55:165-236 (American Geophysical Union, Washington D.C., 1989). Essential introduction to interpretation of increases of CO₂ over the Anthropocene. (I)-(A)

39. “New estimates of radiative forcing due to well mixed greenhouse gases,” G. Myhre, E. J. Highwood, K. P. Shine, F. Stordal, *Geophys Res Lett* **25**, 2715–2718 (1998). doi:10.1029/98GL01908. Widely cited expressions for dependence of forcing on mixing ratio. (I)

40. “Radiative forcing by well-mixed greenhouse gases: Estimates from climate models in the Intergovernmental Panel on Climate Change (IPCC) Fourth Assessment Report (AR4),” W.D. Collins, V. Ramaswamy, M.D. Schwarzkopf, Y. Sun, R.W. Portmann, Q. Fu, S.E.B. Casanova, J.-L. Dufresne, D.W. Fillmore, P.M.D. Forster, V.Y. Galin, L.K. Gohar, W.J. Ingram, D.P. Kratz, M.-P. Lefebvre, J. Li, P. Marquet, V. Oinas, Y. Tsushima, T. Uchiyama, and W.Y. Zhong, *J. Geophys. Res.* **111**, D14317 (2006). doi:10.1029/2005JD006713. Detailed examination of radiation transfer models. (A)

41. “Cloud adjustment and its role in CO₂ radiative forcing and climate sensitivity: A review,” T. Andrews, J. M. Gregory, P. M. Forster, and M. J. Webb, *Surveys in Geophysics* **33**, 619-635 (2012). Influential paper examining short-term influences of incremental greenhouse gases on atmospheric structure. (I)

42. “Adjustments in the forcing-feedback framework for understanding climate change,” S.C. Sherwood, S. Bony, O. Boucher, C. Bretherton, P. M. Forster, J. M. Gregory, and B. Stevens, *Bull. Amer. Meteorol. Soc.* **96**, 217-228 (2015). doi:10.1175/BAMS-D-13-00167.1 Good exposition of forcing, adjusted forcing, sensitivity, feedback concepts. (I)

43. “The role of long-lived greenhouse gases as principal LW control knob that governs the global surface temperature for past and future climate change,” A. A. Lacis, J. E. Hansen, G. L. Russell, V. Oinas, and J. Jonas, *Tellus B*, 65 (2013). doi:10.3402/tellusb.v65i0.19734
Accessible treatment of greenhouse effect of long-lived gases and water vapor. (I)

44. “Carbon dioxide and climate impulse response functions for the computation of greenhouse gas metrics: A multi-model analysis,” F. Joos, et al., *Atmos. Chem. Phys.* **13**, 2793-2825 (2013), doi:10.5194/acp-13-2793-2013. Review of impulse-response models for incremental CO₂. (I)

VII. CLIMATE SYSTEM RESPONSE TO FORCING; CLIMATE SENSITIVITY

The key question facing the climate change research community is how much global temperature would be expected to increase for a given increase in CO₂ or other GHGs in the atmosphere. Closely related is attribution of the observed increase in global temperature to the increase in GHGs and whether the magnitude of this increase is consistent with expectation. Yet another key question is the time scale over which such temperature response would occur. Change in GMST is commonly taken as the principal indicator of climate change under the assumption that changes in other components of the climate system would scale linearly with change in GMST. This hypothesis is borne out for global-annual quantities, such as precipitation amount, in studies with global climate models. Computer representations of the key processes of the climate system permit examination of the consequences of perturbations in amounts of greenhouse gases and aerosols or other perturbations (realistic or intentionally unrealistic) such as changing the solar constant. Locally, and over shorter time periods, changes can be quite nonlinear, especially those

associated with the ice-liquid water transition. Here the focus is restricted to GMST as an indicator of climate change on a global scale.

Recognition that a forcing would be expected to induce a change in global temperature leads to definition of a quantity commonly denoted as Earth's equilibrium climate sensitivity, the amount by which GMST would change, for long times, in response to a sustained global mean forcing F , normalized to that forcing,

$$S_{\text{eq}} \equiv \frac{\Delta T_s}{F} \text{ or equivalently } \Delta T_s = S_{\text{eq}} F \quad (7)$$

Equation (7) may also be viewed an explicit statement of the linearity of response of GMST to forcing, at least to first order in the perturbation; see SN7. Determination of this so-called equilibrium sensitivity is a longstanding goal and challenge to the climate research community. It is important here to qualify use of the word "equilibrium" in the context of climate sensitivity. It should be emphasized Earth's climate is by no means an equilibrium system. A state of dynamic equilibrium is characterized by detailed balance (equal and opposite fluxes) on all paths. This condition is decidedly not met by Earth's climate system, which is characterized by shortwave radiation in and longwave radiation out. Nonetheless the term "equilibrium climate sensitivity" is in widespread use; hence the subscript "eq."

Importantly, the equilibrium sensitivity is pertinent to the changes in surface temperature that characterize the response of Earth's climate system to perturbations generally, not just to the hypothetical situation of a new steady state. Let the N be the net energy flux into the system. For the unperturbed system, this net energy flux consists of two terms, the absorbed shortwave flux Q_0 and the emitted longwave flux E_0 , where the subscripts 0 denote the initial, unperturbed state.

In this initial state

$$N_0 = Q_0 + E_0 = 0 . \quad (8)$$

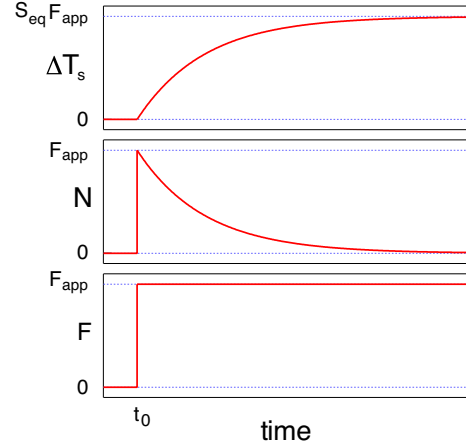
The response of the climate system to a perturbation is illustrated schematically in Figure 10 for the example of a hypothetical step-function perturbation, the application of a constant forcing F_{app} commencing at time t_0 , shown in the bottom panel. Here “external” means that the perturbation is not a part of the climate system, for example the addition of an incremental amount of a greenhouse gas into the atmosphere or, hypothetically, an increase in the solar constant. The change in radiation budget due to the forcing is to be distinguished from the change in the budget that would result from climate system response to the perturbation. With the sign convention that positive forcing F denotes an increase in the net energy flux into the system, then initially, at time immediately after t_0 , the rate of change of the heat content of the planet, N , previously 0, is abruptly increased by the forcing, middle panel,

$$N(t_{0+}) = Q_0 + E_0 + F_{\text{app}} = F_{\text{app}} . \quad (9)$$

The positive net energy flux results in a gradual increase in the heat content of the planet and in turn the surface temperature, top panel. As the temperature increases, the climate system responds by increasing the emitted longwave radiation (decreasing E ; recall the sign convention that E is the negative of the emitted longwave flux) and/or by increasing reflected shortwave irradiance from the planet (decreasing Q , the absorbed shortwave flux). Both of these responses would over time decrease the net downward radiative flux at the TOA, N , offsetting the imposed forcing. This response of the climate system to an imposed forcing is the reason that after time, the energy imbalance of the planet is much less than the applied forcing. A simple, but considerably more realistic, representation of the time response of the climate system to perturbations is given by a two-compartment model of the climate system.⁴⁵⁻⁴⁸ This model exhibits two time constants, a short time constant of about 8 years characteristic of the response

of the ocean mixed layer and a long time constant of about 500 years, characteristic of the response of the deep ocean.

Figure 10. Conceptual depiction as a function of time of response of climate system to step-function forcing at time t_0 . F_{app} is the applied forcing; ΔT_s is the change in surface temperature; N is the rate of change of heat content with time or, equivalently, the net radiative flux imbalance at the top of the atmosphere, TOA.



Under the assumption (SN7) that the decrease in net downward flux at the TOA is linear in the change in surface temperature, then over time subsequent to imposition of the perturbation,

$$N(t > 0) = F_{app} + \left(\left. \frac{\partial Q}{\partial T_s} \right|_0 + \left. \frac{\partial E}{\partial T_s} \right|_0 \right) \Delta T_s(t), \quad (10)$$

where the subscript 0 denotes that the derivatives are evaluated at the initial state, consistent with treatment of effect of the perturbation to first order. At long time such that a new steady state is reached, the net flux into the system $N(t \rightarrow \infty) \rightarrow 0$. At such time

$$\Delta T_s(\infty) = - \left(\left. \frac{\partial Q}{\partial T_s} \right|_0 + \left. \frac{\partial E}{\partial T_s} \right|_0 \right)^{-1} F_{app} \quad (11)$$

so that the identification can be made, cf. Eq. (7):

$$S_{eq} = - \left(\left. \frac{\partial Q}{\partial T_s} \right|_0 + \left. \frac{\partial E}{\partial T_s} \right|_0 \right)^{-1}. \quad (12)$$

Eq. (12), which formally relates the equilibrium climate sensitivity to the derivatives of absorbed shortwave flux and emitted longwave flux with respect to surface temperature, is useful in defining feedbacks in the climate system and as a tool for examining contributions to climate sensitivity in three-dimensional global climate models. The feedback terminology, which derives from its use in analyzing electronic circuits, was introduced into the climate change literature by Hansen et al.⁴⁹ An important insight from Figure 10, and the result holds generally, is that a forcing is not a quantity that can be determined by measurement, for example by measurement of the energy imbalance at the TOA. Rather it is a quantity that can be obtained only by calculation based on knowledge of the perturbation in atmospheric composition, taking into account the state of the atmosphere.

An important insight from Eq. (12) is that the equilibrium sensitivity is a useful measure of climate change not just when the system has attained a new steady state, but generally (*e.g.*, Forster, 2016).⁵⁰ Substituting into Eq. (10) yields

$$\Delta T_s(t) = S_{eq}[F(t) - N(t)] \quad (13a)$$

where $\Delta T_s(t)$ and $F(t)$ are defined relative to an initial steady state. Still more generally, for two states of the climate system, neither of which is at steady state,

$$\Delta T_s = S_{eq}(\Delta F - \Delta N), \quad (13b)$$

where all Δ 's are calculated between the two climate states. These expressions, which rest on conservation of energy in the climate system and which therefore might be considered “the simplest imaginable parameterization of climate system response to radiative forcing,*” are central to interpretation of climate change. In contrast to forcing, the energy imbalance of the climate system N is a quantity that can be measured, in principle at the TOA from satellites and

in practice as the rate of change of global heat content, the great majority of which is manifested in change in temperature of the global ocean.⁵¹

*I thank Bjorn Stevens for the phrase.

An initial indication of the equilibrium sensitivity of Earth's climate to a radiative perturbation may be gained from the model of the climate system given by Eqs. (1)-(3) without feedbacks. In the absence of feedbacks, that is, neither the planetary co-albedo, γ , nor the effective emissivity, ε , (§II) is a function of surface temperature, T_s , the derivatives in Eq. (11) are

$$\frac{\partial Q}{\partial T_s} = 0; \quad \frac{\partial E}{\partial T_s} = -4\varepsilon\sigma T_s^3 = -\frac{4}{T_s}\varepsilon\sigma T_s^4 = -\frac{4}{T_s}\frac{\gamma J_S}{4} = -\frac{\gamma J_S}{T_s}, \quad (14)$$

from which the sensitivity of this no-feedback climate system, denoted by the subscript NF, is

$$S_{\text{NF}} = \frac{T_s}{\gamma J_S}. \quad (15)$$

This no-feedback sensitivity is the equilibrium sensitivity of a Stefan-Boltzmann-like planet that is gray in both the shortwave (co-albedo $\gamma = 0.71$) and the longwave (emissivity $\varepsilon = 0.62$) but with both grayness quantities held constant is about $0.30 \text{ K}/(\text{W}\cdot\text{m}^{-2})$. If the assumptions of this model were accurate for Earth, we would have solved a big part of the science question having to do with climate change. Unfortunately, the problem is much more complicated than this because the actual response of Earth's climate system to perturbations includes the effects of feedbacks.

Historical understanding of Earth's actual "equilibrium" climate sensitivity is summarized in Figure 11, which shows best estimates of this quantity and of associated uncertainties going back to the original estimate by Arrhenius⁵² (Nobel Prize in chemistry for ionic dissociation; activation energy of chemical reactions). Arrhenius obtained his estimate by extensive

calculations as a function of latitude and season, taking into account snow/ice cover, relative humidity, cloudiness, and the absorption spectra of water vapor and carbon dioxide. Also shown for reference is the no-feedback sensitivity just calculated, with the date being that of the determination of Stefan's constant. (There is no indication that Stefan calculated this sensitivity, but he did use his law to obtain a very accurate determination of the temperature of the Sun⁵⁴) Despite much work, especially over the past several decades, Earth's equilibrium sensitivity remains quite uncertain, for a variety of reasons, as summarized in the 2013 IPCC Assessment (Ref. [4], §TFE.6). As the value of this sensitivity has major implications on strategies to constrain global temperature rise due to increases in GHG concentrations, determination of Earth's climate sensitivity is the "holy grail" of current climate change research.

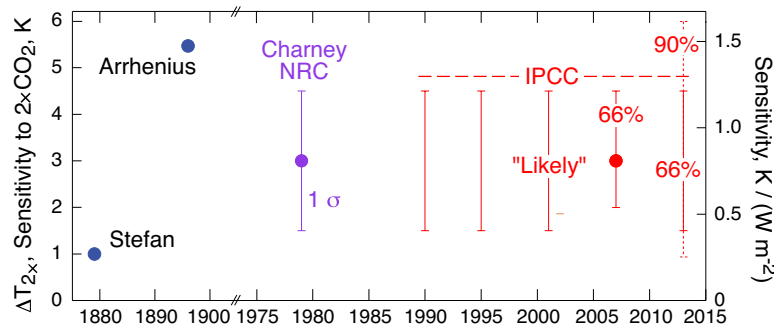


Figure 11. Historical estimates of Earth's "equilibrium" climate sensitivity. Sensitivities are given as long-term temperature increase ΔT_{2x} , left axis, that would result in response to sustained doubling of atmospheric CO_2 and in systematic units, $\text{K}/(\text{W}\cdot\text{m}^{-2})$, right axis, with the conversion (forcing due to doubled CO_2) taken as $3.7 \text{ W}\cdot\text{m}^{-2}$. The value denoted Stefan represents the no-feedback sensitivity calculated, Eq. (15), using the Stefan-Boltzmann radiation law but was not actually calculated by Stefan. The value denoted Arrhenius is by direct calculation (Arrhenius, 1896).⁵² Charney NRC is from an assessment by the U. S. National Research Council (Charney et al., 1979).⁵³ The several ranges (central 66% of the likelihood distribution) and, for 2007, point and range, in red are best estimates in the several reports of the Intergovernmental Panel on Climate Change, IPCC; also shown for 2013 is central 90% range, dashed.

Attention is called to the two ordinate scales on the graph in Figure 11. For historical reasons that go back to Arrhenius' 1896 estimate, the sensitivity of the climate system to a radiative

perturbation is commonly expressed as long-term temperature increase $\Delta T_{2\times}$ that would result from a sustained doubling of atmospheric CO_2 , denoted here and elsewhere as the CO_2 *doubling temperature* of the planet. This quantity is also commonly denoted the “equilibrium climate sensitivity” of the planet, but as stressed above the system is not an equilibrium system and the quantity is a temperature change for a specific forcing, not a sensitivity. Expressing the long-term sensitivity as $\Delta T_{2\times}$, denominated on the left-hand axis of the figure, particularizes the sensitivity as the response to CO_2 doubling; this particularization raises questions, for example, about possible dependence on the magnitude of CO_2 mixing ratio at the initial state and about the response to a perturbation other than that of doubling CO_2 (other magnitudes of CO_2 perturbation or other kinds of radiative forcings). The systematic unit for sensitivity, $\text{K}/(\text{W}\cdot\text{m}^{-2})$, as determined in the above calculation for the no-feedback climate sensitivity and denominated on the right-hand axis, has not gained much traction, much as it might seem to be preferred. The conversion between the two quantities is

$$\Delta T_{2\times} = F_{2\times} S_{\text{eq}}, \quad (16)$$

where $F_{2\times}$ denotes the forcing that would result from doubling atmospheric CO_2 , commonly taken as $3.7 \text{ W}\cdot\text{m}^{-2}$ (Table 1; Ref [39]). If $F_{2\times}$ were accurately known, then converting between doubling temperature $\Delta T_{2\times}$, unit K, and sensitivity S_{eq} , unit $\text{K}/(\text{W}\cdot\text{m}^{-2})$, would pose no problem. However the central 90% uncertainty range in the radiative forcing by doubled CO_2 , as given in the most recent (2013) IPCC Assessment, [$\pm 20\%$] (Ref [4], Technical Summary §TFE4), is substantial.

All of the estimates of Earth’s equilibrium climate sensitivity shown in Figure 11 and virtually all current estimates exceed the no-feedback sensitivity and are therefore indicative of positive

feedback in the climate system. The best estimate and range denoted “NRC”⁵³ comes from an assessment conducted under the auspices of the National Research Council of the United States that was informed largely by early calculations with GCMs, general circulation models of Earth’s atmosphere. Although remarkable for their time, the models of that time were quite primitive by the standards of today’s climate models. The several ranges and, for the 2007 assessment, best estimate and range, of the successive Assessment Reports of the IPCC are based on considerations of multiple sources of information: GCM calculations, energy balance estimates, and estimates from paleo climates. Also shown in Figure 11 is the estimate of the central 90% of the likelihood distribution for climate sensitivity given in the 2013 Assessment, the lower end of which coincides with the no-feedback sensitivity.

As a summary of the present state of understanding of Earth’s climate sensitivity, Figure 11 might be viewed as “good-news, bad-news.” The good news is that the best estimates given in the several studies and assessments are all about the same. The bad news is that the present estimate of this sensitivity is uncertain to a factor of 3, where the uncertainty range represents the central 66% of the likelihood distribution, approximately $\pm 1 \sigma$. Further bad news is that despite all the intervening research, the estimates of the uncertainty range have not diminished between the 1979 NRC report and the 2013 IPCC report. This uncertainty thus remains quite large relative to the accuracy, say 25%, required to develop emission control strategies to limit the future increase in GMST to a particular desired value.

An important point pertinent to quantifying past and prospective climate change has to do with the small magnitudes of the changes in radiative fluxes and global temperature relative to the magnitudes of the initial, unperturbed quantities. The observed change in GMST of about 0.8 K (Ref. [4], §2.4) represents a change of about

0.3% relative to the initial 287 K. Even the 2 K increase in GMST that is widely considered a threshold of dangerous anthropogenic interference with the climate⁵⁵⁻⁵⁷ and which is the target maximum increase in temperature specified in the 2015 Paris Agreement of the United Nations Framework Convention on Climate Change (https://unfccc.int/files/meetings/paris_nov_2015/application/pdf/paris_agreement_english_.pdf) represents a change in GMST of less than 1%. The challenge to the climate change research community is to gain quantitative understanding of the changes in quantities influencing climate change and the expected response of the system to the accuracy necessary for informed decision making regarding prospective controls on future emissions of climate influencing substances. Such quantitative understanding is essential to answering “what if” questions regarding the consequences of future emissions of climate influencing substances. Determining the increase in GMST that would result if the mixing ratio of CO₂ were to increase to twice its preindustrial value to some desired level of accuracy, say 25%, is a daunting challenge.

45. “Vertical heat transports in the ocean and their effect on time-dependent climate change,” J. M. Gregory, *Clim. Dyn.* **16**, 501–515 (2000). Important paper examining time scales of climate system response to perturbations. (I).

46. "Implications of delayed actions in addressing carbon dioxide emission reduction in the context of geo-engineering," O. Boucher, J. A. Lowe, and C. D. Jones, *Climatic Change* **92**, 261-273 (2009). Exposition of two-time-constant model and application via convolution of impulse response function with prospective forcings. (E).

47. “Probing the fast and slow components of global warming by returning abruptly to preindustrial forcing,” I. M. Held, M. Winton, K. Takahashi, T. Delworth, F. Zeng, and G.

K. Vallis, *J. Clim.* **23**, 2418–2427 (2010). Influential study with general circulation model and simple model. (I)

48. “Determination of Earth’s transient and equilibrium climate sensitivities from observations over the twentieth century: Strong dependence on assumed forcing,” S. E. Schwartz, *Surveys Geophys.* **33**, 745-777 (2012). Analysis using two-compartment climate model. (E) - (I).

49. “Climate sensitivity: Analysis of feedback mechanisms,” J. Hansen, A. Lacis, D. Rind, G. Russell, P. Stone, I. Fung, R. Ruedy, J. Lerner, in **Climate Processes and Climate Sensitivity**, J.E. Hansen and Takahashi T (editors), AGU Geophysical Monograph 29. American Geophysical Union, pp 130-163 (1984). Accessible; highly influential paper. (I)

50. “Inference of climate sensitivity from analysis of Earth’s energy budget,” P. M. Forster, *Annu. Rev. Earth Planet. Sci.* **44** 85–106 (2016). doi: 10.1146/annurev-earth-060614-105156. Good recent review. (E)

51. “An imperative to monitor Earth’s energy imbalance,” K. Von Schuckmann, M. D. Palmer, K. E. Trenberth, A. Cazenave, D. Chambers, N. Champollion, J. Hansen, S. A. Josey, N. Loeb, P.P. Mathieu, and B. Meyssignac, *Nature Climate Change* **6**, 138-144 (2016). Important recent overview. (I)

52. “On the Influence of carbonic acid in the air upon the temperature of the ground,” S. Arrhenius, *Phil. Mag. S.5* **41** (251) 237-276 (1896). Historically important; defined the problem of climate system response to doubling of CO₂. (I)

53. “Carbon dioxide and climate: A scientific assessment,” J. G. Charney, A. Arakawa, D. J. Baker, B. Bolin, R. E. Dickinson, R. M. Goody, C. E. Leith, H. M. Stommel, and C. I. Wunsch Natl. Acad. Sci., 22 pp. Washington, DC. (1979). Available at: http://download.nap.edu/cart/download.cgi?record_id=12181. Influential summary of state of knowledge at the time. (E)

54. “Über die Beziehung zwischen der Wärmestrahlung und der Temperatur,” J. Stefan, Sitz. Math. Naturwiss. Cl. Kais. Akad. Wiss. **1**, 391–428 (1879). <http://www.ing-bueroebel.de/strahlung/Original/Stefan1879.pdf>. Historically important discovery of a key physical law. (E)

55. “Report of the Conference of the Parties on its fifteenth session, held in Copenhagen from 7 to 19 December 2009. Addendum Part Two.” United Nations Framework Convention on Climate Change. (2010). <http://unfccc.int/resource/docs/2009/cop15/eng/11a01.pdf>. Historically important statement of international concern over the consequences of the intensified greenhouse effect. (E)

56. “Dangerous anthropogenic interference, dangerous climatic change, and harmful climatic change: non-trivial distinctions with significant policy implications,” L. D. Harvey, Climatic Change, 82, 1-25 (2007). P; (E)

57. “Increasing impacts of climate change upon ecosystems with increasing global mean temperature rise,” R. Warren, J. Price, A. Fischlin, S. de la Nava Santos, and G. Midgley, Climatic Change, 106, 141-177 (2011). Assessment. (E)

VIII. INFERENCES AND IMPLICATIONS

Knowledge of the forcing over the Anthropocene together with Eq. (13b) relating forcing to expected change in global mean surface temperature serves as the basis for comparison of expected and observed change in GMST. The observed increase in GMST over the period of globally representative instrumental measurements from the second half of the 19th century to 2011 given by the 2013 IPCC Assessment (Ref. [4], §2.4.3) was about 0.8 K (<https://crudata.uea.ac.uk/cru/data/temperature/HadCRUT4-gl.dat>). The best estimate total forcing over the period 1850-2011 is $2.2 \text{ W}\cdot\text{m}^{-2}$ (Figure 8). The present planetary heating rate inferred from increase in the heat content of the planet over time, N , also taken from the 2013 IPCC Assessment (Ref. [4], Box 3.1) is about $0.5 \text{ W}\cdot\text{m}^{-2}$. For the equilibrium climate sensitivity expressed as CO₂ doubling temperature $\Delta T_{2\times}$ taken as the central value of the 2013 IPCC estimate, 3 K, and the forcing of doubled CO₂ taken as $3.7 \text{ W}\cdot\text{m}^{-2}$, the calculated increase in GMST, 1.4 K is substantially greater than the observed increase. This discrepancy is shown graphically in Figure 12, which shows the increase in GMST calculated by Eq. (13b) with $N = 0.5 \text{ W}\cdot\text{m}^{-2}$ as a function of total forcing and equilibrium climate sensitivity (expressed as $\Delta T_{2\times}$). The calculated increase in GMST, 1.4 K, falls well to the right of the observed value $\Delta T = 0.8 \text{ K}$ denoted by the thick contour line. However, the discrepancy is readily resolved within present uncertainties in forcing and climate sensitivity as the contour denoting the observed increase in GMST 0.8 K can be achieved by a wide-ranging mix of forcing and climate sensitivity within their respective uncertainties denoted by the vertical and horizontal pairs of lines. Thus the observed increase in GMST can be achieved for $\Delta T_{2\times}$ at the low end of the range given by the 2013 IPCC Assessment, 1.5 K, if the total forcing is $2.5 \text{ W}\cdot\text{m}^{-2}$ or, alternatively, for $\Delta T_{2\times}$ at the high end of the IPCC range, 4.5 K, if the total forcing is $1.1 \text{ W}\cdot\text{m}^{-2}$, or anywhere in-between.

Indeed, if the forcing is at the high end of the IPCC range, $3.3 \text{ W}\cdot\text{m}^{-2}$, $\Delta T_{2\times}$ must be 1 K, a very low sensitivity, essentially equal to the no-feedback sensitivity (Figure 11). On the other hand, if the forcing is at the low end of the uncertainty range, $1.3 \text{ W}\cdot\text{m}^{-2}$, then $\Delta T_{2\times}$ must be 5 K, quite a high sensitivity. This analysis shows that the present uncertainty in total forcing precludes observationally constraining climate sensitivity, and vice versa.

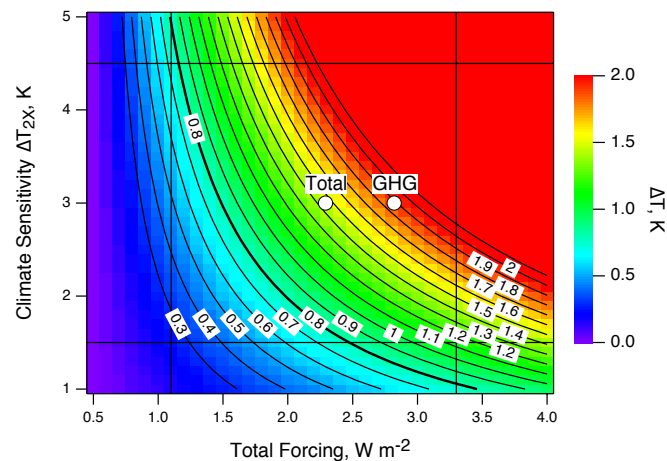


Figure 12. Dependence of expected increase in global mean surface temperature (accounting for global heating rate of $0.5 \text{ W}\cdot\text{m}^{-2}$) on total forcing over the Anthropocene, abscissa, and equilibrium climate sensitivity expressed as long-term temperature increase $\Delta T_{2\times}$ that would result in response to sustained doubling of atmospheric CO_2 , ordinate. Vertical black lines denote central 90% of the likelihood distribution of forcing and horizontal lines denote central 66% of the likelihood distribution of climate sensitivity, both as given by the 2013 IPCC Assessment⁴. Bold contour at 0.8 K denotes approximate value of observed increase in GMST. Points denote expected increase in GMST due to IPCC best estimate total forcing over the Anthropocene, $2.29 \text{ W}\cdot\text{m}^{-2}$ and by long-lived greenhouse gases only, $2.82 \text{ W}\cdot\text{m}^{-2}$ (Figure 8).

This situation has major implications regarding developing strategies to limit climate change. Importantly, reducing fossil fuel combustion to limit CO_2 emissions would also reduce emissions of aerosols and precursor gases. As the atmospheric residence time of these aerosols is quite short (weeks) relative to that of CO_2 and other greenhouse gases (decades to centuries), reducing fossil fuel emissions would thus result in a rapid decrease of the negative aerosol forcing. In turn total forcing and GMST would increase. Under this situation, the total forcing would

increase, in the limit, to the present forcing by long-lived GHGs, $2.8 \text{ W}\cdot\text{m}^{-2}$, denoted "GHG" in Figure 12. For climate sensitivity at its best estimate value the resulting temperature increase relative to preindustrial would be 1.9 K. Within present uncertainty in climate sensitivity, as given by the 2013 IPCC Assessment,⁴ the temperature increase above preindustrial to which the planet is committed on account of long-lived GHGs now in the atmosphere would range from the 1 K already realized to, at the high end of the sensitivity range, as great as 2.8 K. The latter substantially exceeds the widely accepted 2 K threshold for dangerous anthropogenic interference with the climate system (§VII). The possibility that the negative forcing by anthropogenic aerosols has prevented the increase in GMST that would otherwise have been much greater has been characterized as a "Faustian bargain."⁵⁸ To forestall the full impact of the incremental GHGs, the aerosol offset or some other form of geoengineering would need to be maintained long after the benefit gained from combustion of fossil fuels has been enjoyed.

With respect to societal decision making on future emissions of CO₂ and other greenhouse gases the consequences of the present uncertainties are quite discomfiting. If climate sensitivity is at the low end of the uncertainty range, then perhaps there is time for an orderly transition from reliance on fossil fuels as the primary source of the world's energy to alternative sources of energy. If, however, climate sensitivity is at the high end of that range, then future emissions will add to the already committed increase in GMST that is already well beyond the 2-K threshold that is considered to represent the onset of dangerous interference with Earth's climate.

58. "Sun and dust versus greenhouse gases: An assessment of their relative roles in global climate change," J. E. Hansen, and A. A. Lacis, *Nature* **346**, 713-719 (1990). Important assessment of the consequences of aerosol forcing and the greatly differing accommodation times of aerosols and GHGs; (E)

IX. SUMMARY

This article has reviewed the so-called greenhouse effect of trace species in the atmosphere, water vapor, CO₂ and other polyatomic molecules that absorb and radiate in the thermal infrared, and clouds, calling attention to pertinent primary and secondary literature. The greenhouse effect is a key element of Earth's climate system responsible for a global mean surface temperature, average roughly 287 K, much greater than the radiative temperature at the top of the atmosphere, 255 K. Because of human activities, largely fossil fuel combustion, but including also deforestation, agricultural activities, and other industrial activities, amounts of long-lived greenhouse gases in the atmosphere, have increased substantially relative to their preindustrial values. The radiative forcing of the incremental greenhouse gases over the Anthropocene to date, calculation of which rests rather confidently on well-understood molecular properties and well characterized properties of the climate system, is of order 1% relative to top-of-atmosphere fluxes, small relative to spatial and temporal variability of these fluxes on a variety of scales. However even a 1% increase in global mean surface temperature, ~3 K, would be of great consequence to human society and natural ecosystems. The uncertainties have enormous implications regarding interpretation of increase in GMST to date, committed future increases in GMST, and policy regarding future emissions of long-lived greenhouse gases.

The physics of the greenhouse effect and more broadly of Earth's climate and climate change is a research field that has attracted many good physicists and continues to present important first-order challenges.

Acknowledgment. This manuscript has been authored by employees of Brookhaven Science Associates, LLC under Contract No. DE-SC0012704 with the U.S. Department of Energy. I am indebted to numerous friends and colleagues for reading and commenting on earlier drafts of this article.

*Supplementary Notes to***The Greenhouse Effect and Climate Change**

Stephen E. Schwartz

SN1. The consequences of a global energy imbalance

Any energy imbalance in a given compartment of the climate system will result in heating (or cooling) of that compartment, the rate of which depends on the heat capacity of the compartment. For the atmosphere as a whole, the specific heat of air of $1 \text{ kJ}\cdot\text{kg}^{-1}\cdot\text{K}^{-1}$ and mass per unit area given by p_{atm}/g , $= 1 \times 10^5 \text{ Pa}/(10 \text{ m}\cdot\text{s}^{-2}) = 1 \times 10^4 \text{ kg}\cdot\text{m}^{-2}$ yield for the heat capacity per unit area of the planet $10^7 \text{ J}\cdot\text{m}^{-2}\cdot\text{K}^{-1}$. For an energy imbalance of $3 \text{ W}\cdot\text{m}^{-2}$, roughly that which has been imposed on the planet by the incremental amounts of atmospheric greenhouse gases over the past two centuries (§V), the resultant rate of temperature change, if the atmosphere were uncoupled to any other compartments of the climate system, would be $10 \text{ K}\cdot\text{yr}^{-1}$. This would be rapid climate change indeed, certainly much greater than any sustained rate of change that has been observed over the instrumental record of the past 150 years (perhaps $0.01 \text{ K}\cdot\text{yr}^{-1}$) or than is evident in paleo records. However, this heating rate is predicated just on the heat capacity of the atmosphere. Clearly, other factors are at play.

As it turns out, the great majority of the effective heat capacity of the climate system is due to water in the oceans; land surface exhibits a much lower specific heat and low thermal diffusivity. A calculation similar to that for the atmosphere can be applied to the mixed layer of the world ocean, which exhibits a depth of about 100 m and covers about 70% of the planetary surface. For specific heat $4 \text{ kJ}\cdot\text{kg}^{-1}\cdot\text{K}^{-1}$ and density of seawater $1000 \text{ kg}\cdot\text{m}^{-3}$, the heat capacity, again normalized to the area of the planet, is about $4 \times 10^8 \text{ J}\cdot\text{m}^{-2}\cdot\text{K}^{-1}$, and the calculated heating rate is reduced to about $0.2 \text{ K}\cdot\text{yr}^{-1}$, still far greater than is consistent with observations. As the mixed layer of the ocean is only weakly coupled to the deep ocean,

this calculation rules out an energy imbalance of this magnitude. Hence, the climate system and its several compartments must be considered to be in very close energy balance.

How then is this calculation to be reconciled with a radiative forcing by incremental GHGs of about $3 \text{ W}\cdot\text{m}^{-2}$? Several factors contribute. An increase in surface temperature increases emission of longwave radiation to space, §VII. Some of the increased heat of the ocean mixed layer is conducted to the deep ocean, §VII. And longwave forcing by incremental GHGs is almost certainly offset to some extent by shortwave forcing by anthropogenic aerosols, §V.

SN2. Why are water vapor and carbon dioxide strongly infrared-active whereas nitrogen and oxygen are not? The roles of quantum mechanics

Absorption and emission of electromagnetic radiation by a molecule are manifestations of transitions between quantum states, increasing or decreasing the energy of the molecule, respectively. As the energy states of the molecule are quantized, radiation can be absorbed or emitted only at discrete values of frequency (or wavelength) that correspond to the differences in energies of the initial and final quantum states. The energy range of the terrestrial thermal infrared, Figure 1, coincides with the energy of transitions between vibrational levels within the ground electronic states of molecules.

The above considerations apply not only to the GHGs in Earth's atmosphere, importantly water vapor, carbon dioxide, methane, and nitrous oxide, which are present in trace amounts (§ IV) but also to nitrogen (N_2) and oxygen (O_2), the major constituents of Earth's atmosphere. So why are infrared absorption and emission so important for water vapor and CO_2 and other GHGs, but not for N_2 and O_2 ? The answer lies in quantum mechanics. Because of quantum-mechanical considerations, not all transitions between quantum states are allowed. Specifically, for a transition that involves interaction between the molecule and the electric vector of the radiation field, by far the strongest of such

interactions with radiation, the integral of the dipole moment operator over the product of the wave functions of the initial and final states must be non-zero. For a homonuclear diatomic molecule such as N_2 or O_2 , because the dipole moment operator does not depend on the vibrational coordinate, that integral is zero and the transition is forbidden. The same is true for symmetric vibrations of polyatomic molecules (symmetric stretch of CO_2 ; breathing mode of methane). However, for asymmetric vibrations of symmetric molecules and for all vibrations of molecules such as H_2O that have a permanent dipole moment, for all of which the dipole moment varies with the displacement of the nuclei, the molecule can interact with the electric vector of the radiation field, and the transition is allowed. For this reason, these molecules are strong absorbers and emitters of infrared radiation, and their presence in Earth's atmosphere thus gives rise to the greenhouse effect. Infrared absorption is weakly allowed in N_2 and O_2 because of interactions with the electric quadrupole and magnetic dipole moments of the molecules, and because collisions with other molecules contribute to transition dipole moment. These transitions are far weaker than electric dipole transitions; in Earth's present atmosphere the magnitudes of the greenhouse effect of O_2 and N_2 , even given their much greater abundance, are about 1% of that of CO_2 .^{S1}

If the vibrational transitions take place between discrete quantum states, why are the infrared spectra spread over wide wavelength regions rather than consisting of narrow, delta-function-like transitions? Once again, the answer is in quantum mechanics. Because of requirements of conservation of angular momentum, an allowed vibrational transition must be accompanied by a change in rotational state of the molecule by ± 1 quantum of rotational energy. As the energy of the rotational quantum state varies with rotational quantum number J as $J(J+1)$, the rotational transition energy depends on the initial rotational state of the molecule. Hence, in absorption, for $\Delta J = -1$ or $+1$ the transition energy will be less or greater, respectively, than that of the energy of the vibrational transition itself. As the population of molecules in the ground vibrational state is distributed over a large number of rotational states (according to a

Boltzmann distribution over these states), the energy of absorption is spread over a region of energy (frequency or wavelength band, such as is exhibited in Figure 4), instead of the transition being confined to a single frequency that corresponds to the energy of the vibrational transition. In addition to vibrational transitions, for molecules containing hydrogen atoms arrayed about a heavier atom such as oxygen (water), the energies of rotational transitions without change in vibrational quantum state are sufficiently great as to contribute to absorption and emission at longer wavelengths in the terrestrial thermal infrared. Finally, perturbation of the energies of the individual molecules by collisions with other molecules in the surrounding gas serves to broaden the energies of the quantum states and hence leads to further broadening of the transitions. These spectral broadening processes tend to fill in the gaps in the spectrum between the discrete values of the quantum transitions, thereby increasing the opacity of the atmosphere relative to what it would be if the absorption occurred only in narrow lines with spaces between them like the pickets of a fence with alternating regions of opacity and transmissivity. The smearing of transition energies by interactions with other molecules also greatly enhances absorption and emission of infrared radiation by the condensed-phase water of clouds relative to the much greater abundance of water vapor.

SN3. The physics of the greenhouse effect

The greenhouse effect may be thought of as the net longwave radiative effect of gases (and clouds and, to much lesser extent, aerosols) in the atmosphere, at the surface or at the TOA. It is a consequence of absorption and emission of longwave radiation by an atmospheric constituent and thus depends on the local absorptivity (equal, by Kirchhoff's law, to emissivity) and the local atmospheric temperature. These phenomena are illustrated schematically in Figure S1. Panel *a* shows the situation first in the absence of an infrared-active gas in the atmosphere. Thermal radiation is emitted at the surface; as there is no absorption or emission in the atmosphere, the upwelling longwave irradiance at the TOA is equal

to the irradiance emitted at the surface. Panel *b* introduces a hypothetical downwelling emission source at the TOA at the same temperature as the surface, but still without an infrared-active gas in the atmosphere. Because the emitted flux from this hypothetical source is equal and opposite to the emitted flux at the surface there is no net irradiance at the TOA. As all fluxes are matched by equal fluxes in the opposite direction, the system is in a state of dynamic equilibrium. The hypothetical source at the TOA is maintained in panel *c*, to which a slightly absorbing infrared-active trace gas has been added to the atmosphere; here the entire system is isothermal at the surface temperature, and the system is still one of equilibrium. (The condition of the gas being optically thin is not essential here, but it avoids the complication of the radiation emitted by the gas being subsequently absorbed during its traverse through the atmosphere.) Radiation emitted at the surface is absorbed as it traverses the gas, diminishing this flux. At the same time, the gas is emitting a flux in the upward direction that is equal to the absorbed flux. This emitted flux cancels the decrease in upward flux due to absorption, so that the total upward irradiance is a constant with height. The same happens with the downward irradiance; the component of the downward irradiance from the hypothetical source is decreased by absorption, in exactly the same amount as the absorption of the upward flux. As with the upward flux, this absorption is compensated by a downward emitted flux from the gas, so that the total downward irradiance is constant with height as well. The net irradiance is zero at all heights, as it must be for an equilibrium system (equal and opposite fluxes on all paths).

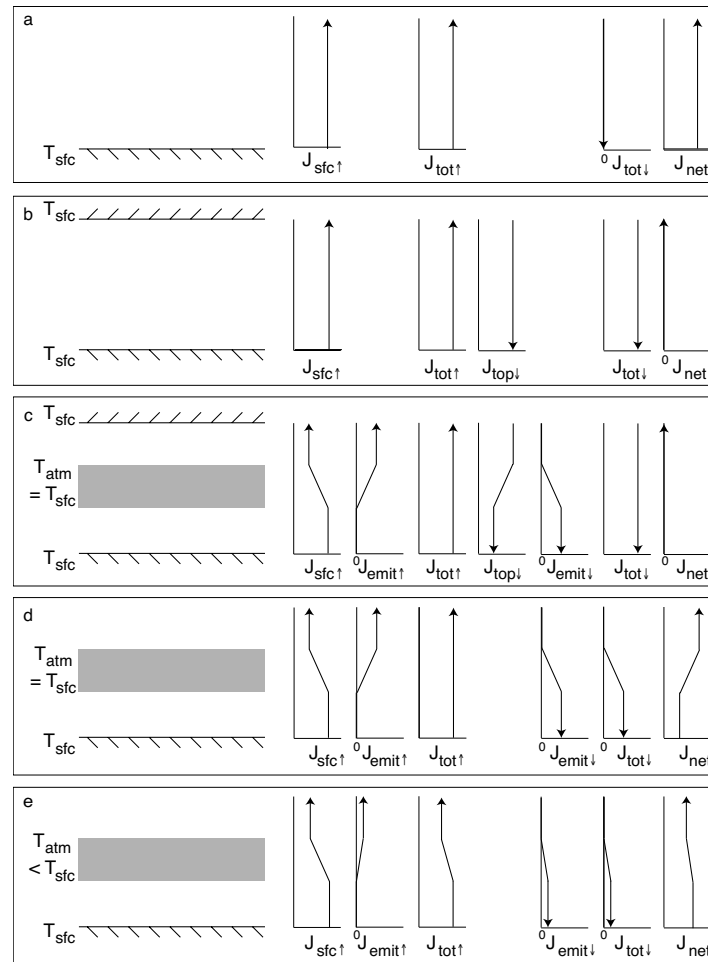


Figure S1. Absorption and emission of thermal infrared radiation for situations denoted by sketches at left: *a*, No absorbing gas. *b*, No absorbing gas, but with hypothetical downward-emitting surface at top of atmosphere at temperature of surface. *c*, As *b*, but with absorbing gas, denoted by gray band, present at temperature T_{sfc} . *d*, As *c*, but no emitting surface at top of atmosphere. *e*, As *d*, but gas is at temperature T_{atm} less than T_{sfc} . For each situation longwave radiative fluxes are shown schematically as function of height in atmosphere, vertical axis. The horizontal axis indicates the magnitude of the several components of flux J : upwelling (\uparrow) or downwelling (\downarrow), emanating from surface (sfc), emitted by gas (emit), or emanating from hypothetical downward-emitting surface at the top of the atmosphere (top); total upwelling or downwelling (tot); and net, upwelling minus downwelling; T denotes temperature at surface (sfc) or in atmosphere (atm).

In panel *d*, the infrared-active gas is still at the temperature of the surface but the hypothetical source at the TOA is no longer present. The upwelling irradiance is the same as in panel *c*, (and indeed as in all the preceding panels) as this upwelling irradiance is unaffected by the downwelling irradiance; the

absorption is compensated by emission so that the total upwelling flux is constant with height. There is no downwelling irradiance from the top but there is still a downward component of the irradiance emitted by the gas, the same as in panel *c*, as this emitted irradiance does not depend on the irradiance from the top but is a consequence only of the emission properties of the gas. The downward emitted irradiance is equal to the upward emitted irradiance, which in turn is equal to the decrease in the upwelling flux from the surface due to absorption. Consequently, there is a component of downwelling irradiance at the surface that would not be present in the absence of the gas (compare panel *b*), and a resultant decrease in the net irradiance leaving the surface. Thus in this isothermal situation there is a surface greenhouse effect but no greenhouse effect at the TOA. It might be observed that more energy is exiting the system, than is entering it. Where does this energy come from? It is drawn from the heat reservoir of the atmosphere; the net radiation by the trace infrared-active gas thus exerts a cooling effect locally. The situation is commonly characterized as one of local thermodynamic equilibrium. It is near thermodynamic equilibrium, but it is not a true equilibrium, as fluxes are not equal and opposite on all paths; it is a steady state. As the GHGs are extracting energy from the surrounding heat bath they must be (very slightly) cooler than the non radiatively active gases that comprise the bulk of the local atmosphere.

Finally, panel *e* depicts the non-isothermal situation, in which the infrared-active gas, higher in the atmosphere than the surface, is at a temperature lower than that of the surface. The absorption of surface irradiance is exactly the same as in panels *c* and *d* as the absorption does not depend on the temperature of the gas. However, as the temperature is lower than in those cases, the thermal emission by the gas is reduced and no longer fully compensates the absorption of upwelling surface irradiance. Consequently there is a reduction in the upwelling irradiance at the TOA from what it would be if the gas were at the same temperature as the surface (*d*) or if the gas were entirely absent (*a*); this is the top-of-atmosphere

greenhouse effect. Emission from the gas in the downward direction is likewise less than in the isothermal situation; the net irradiance from the surface is still diminished from what it would be in the absence of the gas (*a*) but not so much as in the isothermal situation (*d*). The net effect of the absorption and emission of radiation is local radiative cooling of the atmosphere, or at a temperature sufficiently low that emission is less than the power absorbed from below, radiative heating of the atmosphere. In the real world, maintaining steady state in the system requires that the energy that is radiated from the atmosphere in the longwave be restored. This is achieved in the troposphere mainly by convection of latent and sensible heat and in the stratosphere mainly by absorption of shortwave energy.

SN4. Calculation of radiative forcing by an incremental greenhouse gas

As noted in SN3, the TOA greenhouse effect consists of two components: the decrease in outgoing longwave radiation due to absorption of irradiance by the greenhouse gas and the increase in this radiative flux due to emission by the gas. Here expressions are developed for these effects for an optically thin absorbing gas and are applied to evaluate the forcing by CCl_2F_2 as a readily developed example. CCl_2F_2 (dichlorodifluoromethane) is a synthetic gaseous compound that had been widely manufactured and used as a refrigerant and for other purposes until it became recognized by Molina and Rowland^{S2} (Nobel Prize in chemistry, 1995) that chlorine atoms and molecular free radicals, produced in the stratosphere through photolysis by ultraviolet radiation, catalyzed the destruction of ozone, with many attendant consequences. Manufacture of this compound (and also of CCl_3F) was largely banned under the Montreal Protocols,^{S3} but because of their long residence times these compounds are persistent in the atmosphere, and their amounts are only slowly decreasing. As polyatomic molecules, these compounds exhibit numerous radiatively active vibrational transitions in the thermal infrared. Importantly, several of these transitions occur in the so-called “window region” of the infrared spectrum ($\sim 800 - 1000$ and $\sim 1200 - 1300 \text{ cm}^{-1}$; Figure 4) in which there is little absorption by the major infrared

absorbing gases, water vapor or carbon dioxide, and in which, therefore, infrared radiation from the surface is transmitted to space, relatively unimpeded. This situation greatly enhances the greenhouse effect of these gases relative to what it would be in other spectral regions, and greatly simplifies calculation of the magnitude of this effect. An example of such a calculation is presented here.

For any absorption line or band, the rate of absorption of radiant energy is calculated as the product of the absorption coefficient times the incident irradiance integrated over the frequency range $d\nu$ for which there is appreciable absorption. For the incident irradiance at frequency ν given by the Planck function $J_{\text{sfc},\nu}(\nu, T_{\text{sfc}})$ at the surface temperature T_{sfc} , the volumetric rate of absorption of upwelling radiant energy at a given altitude z is

$$P_{\text{abs}\uparrow}(\nu, z) = n_i(z) \int J_{\text{sfc},\nu'}(\nu', T_{\text{sfc}}) \sigma(\nu', z) d\nu', \quad (\text{S4.1})$$

where $n_i(z)$ is the number concentration of absorbing molecules of species X_i and where $\sigma(\nu, z)$ is the absorption cross section of the molecule. The absorption cross section is peaked at the center frequency ν of the transition; it is weakly dependent on altitude as a consequence of pressure-dependent collisional broadening of the transition and temperature-dependent Doppler broadening. The integral is taken over frequencies at which there is appreciable absorption cross section. The absorbed power has the unit, $\text{W}\cdot\text{m}^{-3}$; the Planck function is expressed in the unit $\text{W}\cdot\text{m}^{-2}\cdot\text{Hz}^{-1}$, with frequency ν in Hz. For $n_i(z)$ in $\text{molec}\cdot\text{m}^{-3}$, $\sigma(\nu, z)$ has the unit $\text{m}^2\cdot\text{molec}^{-1}$.

As the Planck function is slowly varying with frequency over a given absorption band, it may be pulled out of the integral, yielding

$$P_{\text{abs}\uparrow}(\nu, z) = J_{\text{sfc},\nu}(\nu, T_{\text{sfc}}) n_i(z) \int \sigma(\nu', z) d\nu'. \quad (\text{S4.2})$$

Further, denoting the integral $\int \sigma(\nu', z) d\nu' = S_\nu(\nu, z)$ yields

$$P_{\text{abs}\uparrow}(\nu, z) = J_{\text{sfc}, \nu}(\nu, T_{\text{sfc}}) S_{\nu}(\nu, z) n_i(z). \quad (\text{S4.3})$$

To good approximation the integral over an absorption line or band, the band strength or integrated absorption coefficient $S_{\nu} = \int \sigma(\nu) d\nu$, is independent of pressure and temperature broadening, and hence the altitude dependence of the band strength may be neglected to first order. The integrated absorption coefficient S_{ν} is related to the integrated absorption coefficient determined in laboratory measurements and commonly reported as $S_{\tilde{\nu}} = \int \sigma(\tilde{\nu}) d\tilde{\nu}$ having unit $\text{cm} \cdot \text{molec}^{-1} = \text{cm}^2 \cdot \text{molec}^{-1} \cdot \text{cm}^{-1}$, where $\tilde{\nu}$ denotes wavenumber (unit, cm^{-1}) as $S_{\nu} = S_{\tilde{\nu}} \times 10^{-4} [\text{m}^2 \cdot \text{cm}^{-2}] c [\text{cm} \cdot \text{s}^{-1}] = 2.98 \times 10^6 [\text{m}^2 \cdot \text{cm}^{-1} \cdot \text{s}^{-1}] S_{\tilde{\nu}}$.

The total absorption of upwelling irradiance, per area, in an atmospheric column is given by the integral of Eq. (S4.3) over the height of the column; this is the top-of-atmosphere absorption forcing, the decrease in emitted irradiance at the top of the atmosphere due to absorption by the gas,

$$F_{\text{abs}}^{\text{toa}}(\nu) = J_{\text{sfc}, \nu}(\nu, T_{\text{sfc}}) S_{\nu} \int n_i(z) dz, \quad (\text{S4.4})$$

with unit $\text{W} \cdot \text{m}^{-2}$. For a well-mixed gas $n_i(z) = x_i n_{\text{air}}(z)$ where x_i (mol/mol air) is the mixing ratio and n_{air} is the number concentration of air molecules, so that the integral over height can be replaced by an integral involving the concentration of air molecules

$$F_{\text{abs}}^{\text{toa}}(\nu) = J_{\text{sfc}, \nu}(\nu, T_{\text{sfc}}) S_{\nu} x_i \int n_{\text{air}}(z) dz. \quad (\text{S4.5})$$

The integral in Eq. (S4.5) is the number of molecules of air N_{air} per square meter in the atmospheric column,

$$\int n_{\text{air}}(z) dz = N_{\text{air}} = \frac{p}{m_{\text{air}} g} = N_{\text{air}}^0 p_{\text{sfc}}^0; \quad (\text{S4.6})$$

here m_{air} is the mass of a molecule of air calculated for the average molecular weight (molar mass) of air, $0.029 \text{ kg} \cdot \text{mol}^{-1}$, and p_{sfc}^0 is the surface pressure in systematic units (Pa); for standard pressure p_{sfc}^0

taken as 1 bar (10^5 Pa), $N_{\text{air}}^0 = 2.12 \times 10^{29}$ molec \cdot m $^{-2}$. This yields the rather simple expression for the TOA absorption forcing in terms of surface pressure in bar

$$F_{\text{abs}}^{\text{toa}}(\nu) = J_{\text{sfc},\nu}(\nu, T_{\text{sfc}}) S_{\nu} x_i N_{\text{air}}^0 (p_{\text{sfc}}^{\text{bar}} / \text{bar}). \quad (\text{S4.7})$$

As noted in SN3, it follows from Kirchoff's law that if an infrared-active gas were in an isothermal system at the temperature of the surface, the power emitted by the gas (in each direction, up and down) would be equal to the power absorbed. However, the gas being at altitude higher than the surface, it is also at lower temperature; this dependence of temperature on altitude strongly influences the emitted power. The reduction in emitted power is a consequence of the lower population of molecules in the excited state than would be present at equilibrium at the temperature of the surface. This temperature dependence is given by the Boltzmann factor for the molecular vibrational state responsible for the emission. Hence, the amount by which the rate of emission is less than that if the system were isothermal is given by the factor $\exp[-h\nu(T(z)^{-1} - T_{\text{sfc}}^{-1})/k]$, where $T(z)$ is the local atmospheric temperature, a function of altitude, and where h and k are the Planck and Boltzmann constants, respectively. Thus at a given altitude z in the atmosphere the volumetric rate of emission is

$$P_{\text{emit}\downarrow}(\nu, z) = P_{\text{emit}\uparrow}(\nu, z) = J_{\text{sfc},\nu}(\nu, T_{\text{sfc}}) x_i S_{\nu} n_{\text{air}}(z) e^{-h\nu(T(z)^{-1} - T_{\text{sfc}}^{-1})/k}. \quad (\text{S4.8})$$

The Boltzmann factor governing the emitted power is referenced to the surface temperature because the Planck emission factor is that for the surface temperature. The local volumetric heating rate is the local difference between absorption and emission

$$P_{\text{net}}(z) = P_{\text{abs}\uparrow}(z) - P_{\text{emit}\downarrow}(z) - P_{\text{emit}\uparrow}(z) = P_{\text{abs}\uparrow}(z) - 2P_{\text{emit}\uparrow}(z). \quad (\text{S4.9})$$

There is no contribution from downwelling irradiance because the gas is treated as optically thin and because the atmosphere is otherwise non-absorbing in the wavelength range under consideration here, the window region. The cumulative change in upwelling irradiance due to the presence of the infrared-active gas from the surface to altitude z is given by the vertical integral of the difference in absorbed and upward emitted power; this is the net forcing of upwelling irradiance due to a specific absorption band of species i as a function of altitude,

$$F_{i\uparrow}(\nu, z) = \int_0^z [P_{\text{abs}\uparrow}(\nu, z') - P_{\text{emit}\uparrow}(\nu, z')] dz' = J_{\text{sfc}, \nu}(\nu, T_{\text{sfc}}) S_{\nu} x_i \int_0^z n_{\text{air}}(z') [1 - e^{-h\nu(T(z')^{-1} - T_{\text{sfc}}^{-1})/k}] dz' . \quad (\text{S4.10})$$

The net TOA forcing is given by the integral over the entire height of the vertical column.

Equation (S4.10) permits evaluation of forcing that would result from a given transition of a given infrared-active gas by numerical integration for a particular atmospheric temperature profile, with the requirements that the scene be cloud-free and that the gas be optically thin and that the transition occur in a region of the spectrum that is not obscured by other infrared-active gases. The results of the calculation are illustrated in Figure S2 for the 925 cm^{-1} band of CCl_2F_2 , which is in the window region of the thermal infrared, Figure 4. The band strength, based on laboratory measurements,^{S4} $S_{\nu} = 4.68 \times 10^{-17} \text{ cm} \cdot \text{molec}^{-1}$ corresponds to $S_{\nu} = 1.40 \times 10^{-10} \text{ m}^2 \cdot \text{molec}^{-1} \cdot \text{Hz}$. The atmospheric mixing ratio of the gas x_i is 0.55 ppb (5.5×10^{-10}), Table 1. The vertical temperature profile is taken as that in Figure 5. The resulting heating rate and forcing profiles, Figure S2, show the heating rate negative (i.e., cooling) at low altitude, warming at high altitude, with the absorption contribution to forcing of upwelling irradiance dominant, offset by roughly half by the emission forcing. The net TOA forcing for this vibrational band is $0.067 \text{ W} \cdot \text{m}^{-2}$. The sum of forcings over the several vibrational bands of the molecule, calculated in the same way, gives a total TOA forcing of $0.17 \text{ W} \cdot \text{m}^{-2}$. Although this forcing is in close

agreement with the value given in Table 1, the close agreement must be viewed as fortuitous. The calculation, carried out for an equatorial temperature profile, neglects spatial and temporal variation of surface and atmospheric temperature and as the actual forcing would be expected to be less than that calculated by the simple approach because of obscuration of the forcing by clouds. Nonetheless, this example illustrates the approach to calculation of radiative forcing by incremental greenhouse gases and the vertical profiles of heating and cooling by absorption and emission of radiation by a greenhouse gas.

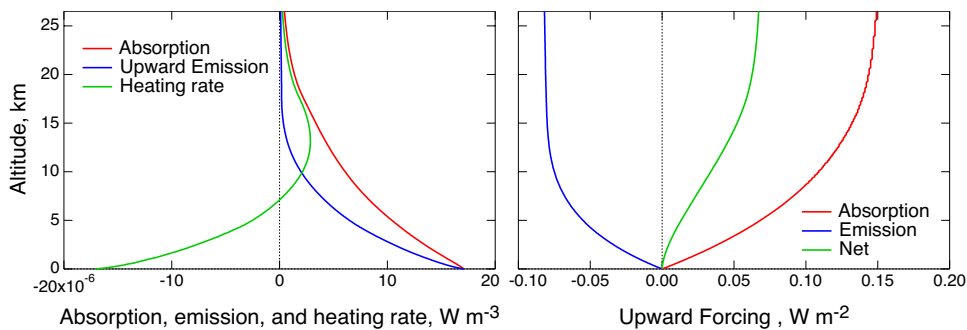


Figure S2. Vertical profiles, *left*, of heating (or cooling, negative) rate and, *right*, of cumulative contribution to TOA forcing by the 925 cm^{-1} band of CCl_2F_2 (positive forcing denotes increase in global heat content). Red curves denote absorption of irradiance emitted at the surface by the infrared-active gas; blue curves denote emission by the gas, and green curves denote the net effect.

SN5. Can forcings from increases in GHGs be measured?

In principle, as the amount of a greenhouse gas is increased in the atmosphere, it should be possible to measure the resultant change in irradiance, at the top of the atmosphere or at the surface. Working against this, however, would be the effects of variation of temperature and water vapor, on a variety of time scales that would exert large fluctuations in infrared power that would overwhelm any change due to the incremental amount of GHG. Moreover, as a consequence of the presence of the incremental amount of GHG, there would, over time, be an increase in surface temperature and resultant increase in thermal infrared emitted at the surface. This would offset the forcing by the incremental GHG, on

account of the increase in surface temperature there would likely be an increase in the temperature and the amount of water in the atmospheric column that would, through the greenhouse effect of water vapor amplify the effect of the initial perturbation (positive feedback). As well, there would likely be changes in the amount and distribution of clouds that would contribute further, with sign that is not yet known, to change in net power at the TOA. Given this situation would it be possible to measure the forcing due to the increment of GHG over a period of time?

If measurements were limited to total broadband thermal infrared, the answer would be a resounding no. However because the several greenhouse gases exhibit unique spectral features, the possibility arises that it might be possible to discern and quantify the changes attributable to increases in individual GHGs from examination of changes in the spectral distribution of the infrared radiation emitted at the TOA. Such an examination^{S5} using 1970 measurements from Nimbus-4 (*cf.* Figure 4) and similar measurements from 1997 reported decreases in emitted radiance in absorption bands of CO₂, CH₄, O₃, chlorofluorocarbons, and also water vapor that were attributed to increases in these gases over this period.

As the greenhouse effect is manifested at the surface as well as at the TOA, secular increases might similarly be expected in downwelling infrared radiance at the surface. Using spectrally resolved measurements at the surface in Oklahoma and at the North Slope of Alaska, Feldman et al.^{S6} examined changes in downwelling irradiance over 2000-2010, during which period CO₂ mixing ratio increased by 22 ppm. Although the observed trends in downwelling radiance were dominated by trends in humidity and temperature, it was possible to account for those trends using measured temperature and humidity profiles as input to a radiation transfer model. This permitted quantification of the increase in downwelling radiance in the wings of the CO₂ absorption bands, where the transitions are not saturated,

consistent with radiation transfer model calculations for the increase in CO₂ over the period. The increase in surface forcing due to the increase in CO₂, calculated as the spectrally integrated increase in downwelling irradiance, was found at both sites to be 0.2 ± 0.06 (1σ) $\text{W}\cdot\text{m}^{-2}\cdot\text{decade}^{-1}$, equivalent to a dependence on CO₂ mixing ratio of 0.010 ± 0.003 $\text{W}\cdot\text{m}^{-2}\cdot\text{ppm}^{-1}$. Radiation transfer model calculations indicated that the increase in the TOA forcing over the period, although somewhat greater than at the surface, was still considerably less than the value in Table 1, 0.016 $\text{W}\cdot\text{m}^{-2}\cdot\text{ppm}^{-1}$.

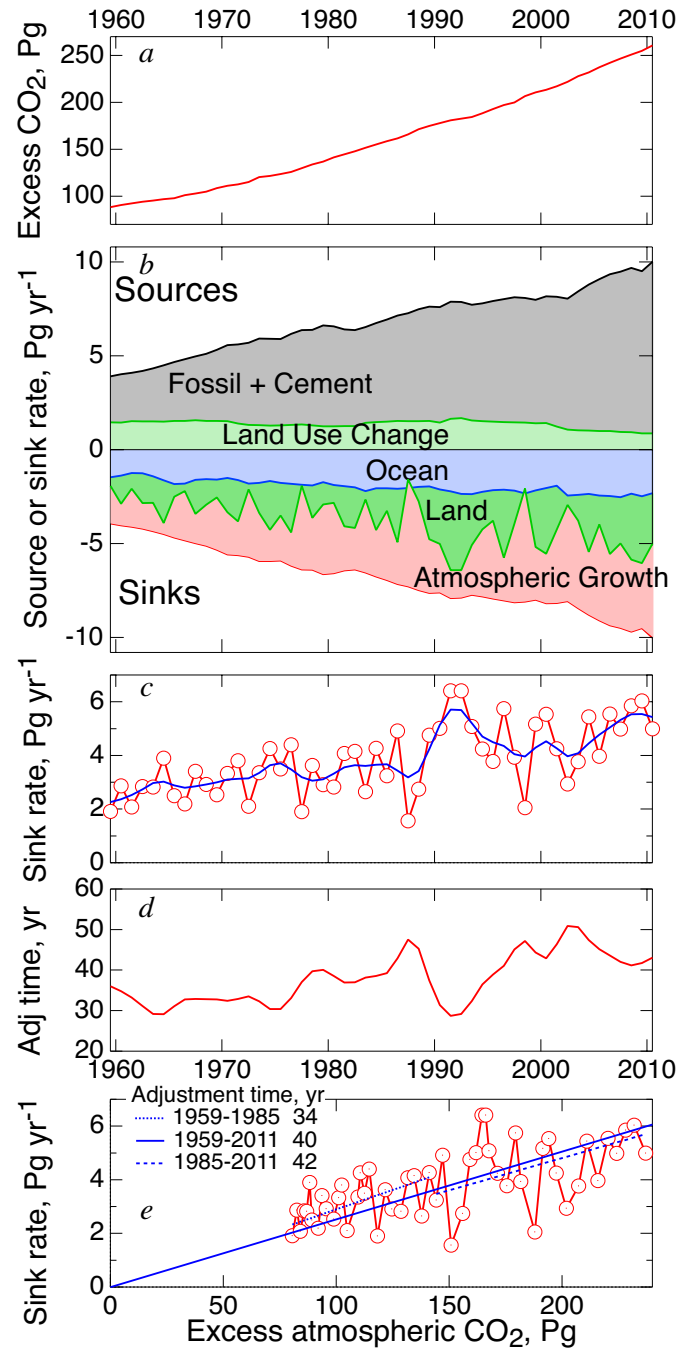
Returning to the question of whether the GHG forcings can be measured, the answer would thus seem to be a qualified yes, but only with use of radiation transfer models to account for other concurrent changes in the temperature and humidity structure that can dominate changes in the longwave irradiance. Nonetheless, the observed changes in the spectral distribution of the radiation lend strong confirmation to the role of incremental GHGs in increasing the greenhouse effect of the planet and to the understanding of the governing processes that is represented in radiation transfer models.

SN6. The budget and adjustment time of incremental atmospheric CO₂

Evaluation of the adjustment time of incremental CO₂ (*i.e.*, in excess of preindustrial) is illustrated in Figure S3 (see also Refs. [S7], [S8]). The amount of excess CO₂ in the global atmosphere (expressed as mass of carbon, as is conventional) in panel *a* is based on contemporaneous measurements, Figure 7; $1 \text{ Pg} = 1 \times 10^{15} \text{ g}$. Panel *b* shows the budget of sources and sinks of CO₂ into/out of the atmosphere. The rate of emissions, at present and historically, is known fairly accurately from inventories of fossil fuel combustion and deforestation; in the aggregate current emissions are about $10 \text{ Pg}\cdot\text{yr}^{-1}$. The principal source of incremental CO₂ at present is fossil fuel combustion, with a further contribution from calcination of limestone in the manufacture of cement; land use change (net of deforestation minus afforestation) contributes about 15% to present global anthropogenic CO₂ emissions. This annual

increment of CO₂ in the atmospheric reservoir is diminished by removal – net uptake by the terrestrial biosphere and transport from the upper ocean to the deep ocean – the rate of which is inferred from observations as the difference between emissions and the annual increase of atmospheric CO₂. The ocean sink was estimated using the average of four global ocean biogeochemistry models forced by observed atmospheric conditions and CO₂ mixing ratio, with the land sink estimated as the residual. The substantial fluctuations in the total annual sink and in the inferred land sink (panel *c*) are not confidently understood. Proportionality of the sink rate to the excess atmospheric CO₂, panel *e*, is consistent with removal of excess CO₂ with a single time constant of about 40 years, evaluated as the inverse of the slope and is consistent with evaluation of this quantity as the ratio of excess atmospheric CO₂ to the sink rate (panel *d*).

Figure S3. *a*, Annual average global excess atmospheric CO₂ based on measurements at Mauna Loa, Hawaii; the unit Pg denotes petagrams (10¹⁵ g) of carbon. *b*, Annual sources and sinks of atmospheric CO₂, 1959-2011 (data from Ref. [S9]; <http://cdiac.ornl.gov/GCP/carbonbudget/2013/>). Sources (positive) and sinks (negative) are shown in summation to categories closer to the *x*-axis. Fossil fuel combustion and cement production are from historical records. Emissions from land use change (net of deforestation and afforestation; Ref. [S10]), are uncertain by 50%. Atmospheric growth is from measurements at Mauna Loa (1959-1980) or global average (1980-2010). *c*, CO₂ removal rate (annual, points, and 3-year smoothing, blue curve) calculated as difference between annual emissions and measured annual atmospheric increment. *d*, CO₂ adjustment time evaluated as excess CO₂ divided by smoothed sink rate. *e*, Sink rate vs. excess CO₂ and linear fits, forced through origin, for entire data set and for first and second halves, indicated by dotted and dashed lines, respectively, with corresponding adjustment times.



It is widely thought (e.g., Refs. [44], [S8]) that well into the future, as the deep ocean becomes increasingly saturated in excess CO₂, the effective rate coefficient for removal of excess CO₂ from the atmosphere–upper-ocean compartment would decrease. Ultimately, at long time (greater than 500 years following a cessation of emission of CO₂ into the atmosphere), the decay of excess atmospheric CO₂

would no longer be characterized by a single time constant but would plateau out at a non-zero value. This can be estimated, based on the solubility of CO₂ and the volume of the deep ocean, as about 20% of the total incremental CO₂ added to the system.

SN7. Treating climate response as linear in the perturbation

How much error results from considering ΔE linear in ΔT_s ? Consider a black body emitting at the global mean surface temperature of Earth, T_s . The emitted flux is

$$E'_{bb} = \sigma T_s^4 \quad (S7.1)$$

where for convenience here the emitted flux is taken here as positive outward. The temperature is increased by ΔT_s , resulting in an increase in the magnitude of the emitted flux ΔE_{bb} . The new emitted flux is

$$E'_{bb} = \sigma (T_s + \Delta T_s)^4 \quad (S7.2)$$

which yields, to second order,

$$\Delta E_{bb} = 4\sigma T_s^3 \Delta T_s \left[1 + \frac{3}{2} \frac{\Delta T_s}{T_s} + L \right]. \quad (S7.3)$$

Consider a 1% perturbation in T_s , about a 3 K increase over the present 287 K. The second term of the quantity in brackets is about 0.015. The take-away message here is that the change in climate that is under consideration is a small perturbation from the initial state, so that the error that results from treating the response as linear is small, at least at the present level of understanding, justifying the treatment of climate system response as linear.

References

[S1] “The natural greenhouse effect of atmospheric oxygen (O₂) and nitrogen (N₂),” Höpfner, M., Milz, M., Buehler, S., Orphal, J. and Stiller, G., *Geophys. Res. Lett.* **39**, L10706, doi:10.1029/2012GL051409 (2012). (I)

- [S2] “Stratospheric Sink for Chlorofluoromethanes: Chlorine atom catalysed destruction of ozone,” Molina, M. J. and F. S. Rowland, *Nature* **249** 810-812 (1974). <http://www.nature.com/nature/journal/v249/n5460/abs/249810a0.html>. Nobel Prize paper. (E)
- [S3] “Stratospheric ozone depletion,” F. S. Rowland, *Phil. Trans. of the Roy. Soc. B: Biological Sciences*, **361**, 769-790 (2006). <http://rstb.royalsocietypublishing.org/content/361/1469/769.short>. Review; (E)
- [S4] “Measurements of the infrared absorption cross-sections of haloalkanes and their use in a simplified calculational approach for estimating direct global warming potentials,” V. L. Orkin, A. G. Guschin, I. K. Larin, R. E. Huie, and M. J. Kurylo, *J. Photochem. Photobiol. A: Chemistry* **157**, 211-222 (2003). <http://www.sciencedirect.com/science/article/pii/S1010603003000571>. (I)
- [S5] “Increases in greenhouse forcing inferred from the outgoing longwave radiation spectra of the Earth in 1970 and 1997,” J. E. Harries, H. E. Brindley, P. J. Sagoo, and R. J. Bantges, *Nature* **410**, 355-357 (2001). <http://www.nature.com/nature/journal/v410/n6826/abs/410355a0.html>. (E)
- [S6] “Observational determination of surface radiative forcing by CO₂ from 2000 to 2010.” D. R. Feldman, W. D. Collins, P. J. Gero, M. S. Torn, E. J. Mlawer, and T. R. Shippert, *Nature* **519**, 339-343 (2015). doi:10.1038/nature14240/ (I)
- [S7] “Greenhouse gas growth rates,” J. Hansen, and M. Sato, *Proceedings of the National Academy of Sciences of the United States of America* **101**, 16109-16114 (2004). <http://www.pnas.org/content/101/46/16109.short>. (E)
- [S8] “What can be learned about carbon cycle climate feedbacks from the CO₂ airborne fraction?” M. Gloor, J. L. Sarmiento, and N. Gruber, *Atmospheric Chemistry and Physics* **10**, 7739-7751 (2010). <http://www.atmos-chem-phys.net/10/7739/2010/acp-10-7739-2010.pdf>. (E)-(I)
- [S9] “Global carbon budget 2013,” Le Quéré, C. et al., *Earth System Science Data* **6**, 235-263 (2014). <https://doi.org/10.5194/essd-6-235-2014>. (E)
- [S10] “Carbon emissions from land use and land-cover change,” R.A Houghton, J.I. House, J. Pongratz, G.R. Van der Werf, R.S., DeFries, M.C., Hansen, C.L. Quéré, and N. Ramankutty, *Biogeosciences* **9**, 5125-5142 (2012). <http://www.biogeosciences.net/9/5125/2012/bg-9-5125-2012.xml>. (E)